

CTH-RF-106

August 1994

**Experiment for Water-Flow Measurement  
by Pulsed-Neutron Activation**

CTH-RF-106

August 1994

**Experiment for Water-Flow Measurement  
by Pulsed-Neutron Activation**

**Krzysztof Drozdowicz<sup>\*)</sup>**

<sup>\*)</sup> *permanent address*

The Henryk Niewodniczański Institute of Nuclear Physics  
ul. Radzikowskiego 152, PL-31-342 Kraków, Poland

Department of Reactor Physics  
Chalmers University of Technology, S-412 96 Göteborg  
ISSN 0281-9775

**Experiment for Water-Flow Measurement  
by Pulsed-Neutron Activation**

*Krzysztof Drozdowicz*

**Abstract**

An experiment is presented which constitutes a feasibility study for applying the neutron activation method for measurement of the water mass transport in pipings, *e.g.* in nuclear power stations. The fast neutron generator has been used as a pulsed-neutron activation source for oxygen in water which circulated in a closed piping system. The  $\gamma$  radiation of the nitrogen product isotope has been measured by the scintillation detectors placed in two positions at the piping. The two time distributions of the pulses have been recorded by a multichannel analyzer (a software design based on CAMAC). The water flow velocity has been estimated from the peak-to-peak time distance. The tests have been performed under different experimental conditions (the neutron pulse duration, the time channel width, the water flow velocity) to define the stability, reproducibility and reliability of the measurement. The detailed results are presented in tables and in time distribution plots. The method has been found useful for the application considered.

## Contents

1. Idea of the measurement .....	5
2. Data acquisition equipment .....	6
3. Software .....	6
<i>Parameters of the multiscalers</i> .....	7
<i>Control of the experiment</i> .....	7
4. Experimental results .....	8
4.0. General explanation .....	8
4.1. Time distribution of the $\gamma$ pulses observed at detector position #0 .....	9
4.2. Time distribution of the $\gamma$ pulses observed from detectors #0 and #1 .....	9
a) <i>Different time parameters of the multiscaler</i> .....	9
b) <i>Comparison of peak shapes</i> .....	10
4.3. Reliability of the measurement .....	11
a) <i>Measurements at water flow <math>v = v_A</math> with <math>\Delta t = 50</math> ms</i> .....	12
b) <i>Measurements at water flow <math>v = v_A</math> with <math>\Delta t = 40</math> ms</i> .....	13
c) <i>Measurements at water flow <math>v = v_B</math> with <math>\Delta t = 40</math> ms</i> .....	14
d) <i>Measurements at water flow <math>v = v_B</math> with <math>\Delta t = 60</math> ms</i> .....	14
5. Conclusions ..	15
Acknowledgements .....	16
References .....	16
List of figures .....	17
Figures .....	18
Appendix A. Documentation of the experiment .....	39
Appendix B. User's manual for program FLW (water flow experiment) .....	42
B.1. Computer files .....	42
B.2. Running the experiment .....	43
B.3. Data treatment .....	43

## 1. Idea of the measurement.

The experiment presented here has been thought as an investigation of a possibility to measure high water-flows in pipings, *e.g.* in nuclear power stations.

The water which flows in a pipe is irradiated by a pulsed 14 MeV neutron source. Oxygen in the water is activated:



with the cross section  $\sigma_A = (40 \pm 3)$  mbarn. The half-life of the product isotope,  $\text{N}^{16}$ , is  $T_{1/2} = 7.352$  s, with  $\gamma$  emission of energies 6.134 MeV (68%) and 7.121 MeV (4.9%) [*e.g.* ALIEV *et al.* 1970].

The time distribution of the  $\gamma$  radiation is measured at a certain distance from the irradiation point. The peak position is assumed to define the time used by the activated water to move from the first to second point. The water flow velocity is found from that time and distance between the two points. A better solution is to use two  $\gamma$  detectors placed at two different points and mea. the time between the two peaks. A water velocity profile is not considered in the simple experiment presented here and the shape of the recorded distribution is not analyzed, which should be done in a more advanced interpretation (*e.g.* BARRET 1982, ZUBER 1986).

The technique of oxygen pulsed activation has been used to measure water flow in geological boreholes (*cf.* SCOTT *et al.* 1993). However, the range of parameters in that experiment (a long activation time of the order of seconds, relatively low velocities) has been quite far from which is expected at the final application of the present experimental idea.

The geometry of the present laboratory measurement is shown in Fig.1. Water circulates in a closed pipe system formed as a rectangle with soft turns. The pulsed neutron source (the 14 MeV neutron generator target) is placed directly at the pipe on one side and the  $\gamma$  detectors are at the perpendicular pipe. This configuration gives a possibility to place concrete shield between the neutron source and the detectors and between the source and a water tank. The tank is used to get a waiting time necessary for the total vanishing of the radiation from the activated amount of water. With a water pump different flow velocities can be achieved (Two velocities have been used in the present experiment). The diameter of the pipe is 10.0 cm. The important distances are:

- detector #0 from target:  $l_0 \approx 150$  cm, measured along the pipe axis,
- detector #1 from target:  $l_1 \approx 245.5$  cm,

detector #1 from det.#0:  $l_{01} = 95.5$  cm (exact).

The  $\gamma$  detectors are in lead shields with openings towards the pipe.

## 2. Data acquisition equipment.

Two independent measuring lines contain  $\gamma$  detectors [the 3"x3" BICRON Model 3M3/3P NaI(Tl) scintillation detector] with HV supplies, photomultipliers, preamplifiers, amplifiers with shaping, discriminators – as shown in Fig.2. The lines are adjusted to give the same amplitude signals.

To create a two-line time analyzer (multiscaler) a CAMAC crate is used with the following modules:

- STARBURST CES computer (PDP11/70 type),
- LeCroy Scaler 4434,
- LeCroy Discriminator 4125A,
- CES Input Output Register 1420,
- CES Histogramic Memory 2161.

## 3. Software.

Multiscalers for the registration of the time distribution of the counts from the detectors are created by a software controlling LeCroy Scaler module 4434. The module contains 32 independent scalers which can be controlled only simultaneously. Two scalers are used for two measuring lines. The multiscaler operating sequence described below runs parallel in both lines. When a single run of the multiscaler is started the pulses are counted by the scaler during a certain time interval, *i.e.* in a time channel, starting from the first channel. When it is finished the counts are immediately written into a buffer register in the module and the scaler is cleared. The next time channel begins, new pulses are counted by the scaler. During this time the data from the register are read by a program, added to the contents which was collected in the first channel during previous runs. Then the procedure is repeated for the second channel, and so on up to the last one. Then, the whole run is repeated a number of times.

The start of the multiscaler run can be delayed after the neutron pulse or can precede it as required. The start pulse for the neutron generator is produced by the program with the Input Output Register CAMAC module.

### *Parameters of the multiscalers.*

Number of lines:	2
Total number of channels in each line:	128 (a choice: 64 or 128)
Time channel width:	from 40 ms, in steps of 1 ms
Delay:	-5000 to +5000 ms

Another option can be used with a one detector line only (Line #0) and with 256 channels.

### *Control of the experiment.*

The experiment is run by the program FLW written specially for this purpose. The program sets by an interactive way the multiscaler parameters (the number of the lines used, the number of the time channels, the channel width, the delay) and other experimental conditions, such as the total number of runs and the neutron pulse repetition time, and parameters for the TD1 display. The required repetition time of the neutron-activation pulses is checked by the program to preset always the time which is not shorter than the interval covered by the multiscaler in a single run.

When the required number of runs is executed the program can either **FINISH** the experiment, or **CONTINUE** with the same or changed number of runs, or switch to a **STAND-BY** status. Then the collected data can be analyzed and a decision can be taken to continue or to finish the experiment.

The **FINISH** command defines the end of the experiment. The collected data, *i.e.* the counts as a function of the channel number (of a given width) are automatically stored in files, separately for each line. Their names are given by the user at the start of the measurement (one to four characters) and are followed by 'F0' or 'F1' for Line #0 or #1, respectively. The input parameter and log files contain 'F0' in their names. See Appendix B ("User's manual") for the details. The data files are created in the same organization as in the TD1 program (unformatted files). This offers the user a possibility to utilize that program for the data analysis. The CES Histogramic Memory module is used during this procedure.

After the experiment **FINISHED**, a new one only can be started even if there has been no change in the experimental conditions (the water flow, the neutron pulsing, the channel width, *etc.*).

#### 4. Experimental results.

##### 4.0. General explanation.

The experiments were performed to assess the suitability of the method for a practical application. Thus, first the time distribution of pulses from detector #0 was investigated. Due to a positive result, the second measuring line, #1, was included. It was found that an estimation of the flow transmit time between the two detectors, based on the peaks of the signal time distributions, is possible. Later, test were performed to observe an influence of the neutron pulse width and time channel width on the results. Measurements to investigate the stability and reproducibility of the system were also performed.

Notations:

$l_L$  – distance,

$t_L$  – time peak position,

$v_L$  – water flow velocity (obtained from the neutron experiment),

where the index

$L = 0$  or  $1$  regarding distance or time between the neutron source and detector #0 or #1, respectively, and

$L = 01$  for quantities between the detectors #0 and #1.

The velocity is calculated as an average:

$$v_L = l_L / t_L \quad (2)$$

The velocity  $v_{01}$  seems to be the most exact one because the distance  $l_{01}$  is along a straight line. A turn of the pipe on the way  $l_0$  (or  $l_1$ ) introduces a perturbation in the water flow and also results in different distances between the source and the detector along stream lines with different radial positions.

$v_F$  – water flow velocity measured with a flow meter,

$T_n$  – duration of the neutron generator pulse,

$\Delta t$  – multiscaler channel width,

$t_m$  – time from the multiscaler start,

$t_d$  – delay time of the multiscaler start (positive or negative),

which gives the real time from the neutron pulse:

$$t = t_d + t_m$$



$c$  – channel compression factor for the TD1 display,  
 $c = 1$  when not specified.

$N_R$  – number of runs (repeated activations).

The collected data (the time distributions) have been analyzed using the TD1 program (see Appendix B).

#### 4.1. Time distribution of the $\gamma$ pulses observed at detector position #0.

The experiment was made using two different widths of the neutron activation pulse ( $T_n = 10$  or  $100$  ms, experiments #785 and #786). Results are plotted in Fig.3. No influence of the  $T_n$  on the distribution peak has been observed. Therefore, in all further experiments the longer pulse,  $T_n = 100$  ms, was used for a stronger activation.

#### 4.2. Time distribution of the $\gamma$ pulses observed from detectors #0 and #1.

##### a) *Different time parameters of the multiscaler.*

Different time parameters were preset for the multiscalers to check the system. The results are plotted in Figs 4 and 5. In experiment #787 (Fig.4) the same observed time range has been preset as in experiment #786. A peak analysis is shown in a corner of the figure. In experiment #788 (Fig.5), a delay of the multiscaler start has been introduced and shorter channels used. Peak positions and the obtained water flow velocities are listed in Table 1.

Differences between the velocities obtained,  $v_0$ ,  $v_1$  and  $v_{01}$ , have been expected as explained in paragraph 4.0.

Differences between the particular velocities  $v_L$  in experiments #787 and #788 have been found corresponding to the differences in peak positions. In both cases the latter difference is smaller than the channel width which sets the time measurement accuracy. An approximate error analysis by the variance of Eq.(2) gives:

$$\sigma^2(v) = \sigma^2(l) (1/t)^2 + \sigma^2(t) l^2 (1/t)^4 \quad (3)$$

Assuming  $\sigma(l) \approx 0$  we get

$$\sigma(v) \approx v \frac{\sigma(t)}{l} \quad (4)$$

The time precision is  $\pm 50$  ms (for channel  $\Delta t=100$  ms) or  $\pm 25$  ms (for  $\Delta t=50$  ms). From this one can assume the standard deviations as  $\sigma(t) \approx 25$  ms or  $\sigma(t) \approx 12$  ms. Then for the length  $l$  on the order of 100 cm and the time  $t_{01} = t_1 - t_0 \approx 1300$  ms an error of the velocity determination is estimated as

$$\sigma(v) \approx 1.4 \text{ cm/s} \quad \text{or} \quad \sigma(v) \approx 0.7 \text{ cm/s}, \quad \text{respectively.} \quad (5)$$

This means that the results for each  $v_L$  of experiments #787 and #788 are fully consistent within this accuracy.

**Table 1.** Test of the consistency of the results while using different parameters of the multi-scaler. ( $T_n = 100$  ms)

Measure- ment #	$t_d$ ms	$\Delta t$ ms	$t_0$ ms	$t_1$ ms	$v_0$ cm/s	$v_1$ cm/s	$v_{01}$ cm/s
787	-1000	100	1992	3315	75.30 $\pm 1.4$	74.06 $\pm 1.4$	72.18 $\pm 1.4$
788	+1400	50	2009	3340	74.66 $\pm 0.7$	73.50 $\pm 0.7$	71.75 $\pm 0.7$

**b) Comparison of peak shapes.**

The amplitude of the distribution from detector #1 (the further one) is lower than from detector #0 (Fig.5) due to the decay of the radiation activity in time and to the diffusion of molecules. The shapes of the peaks after a normalization of the amplitudes are compared in Fig.6. The expected broadening of peak #1 in respect to #0 is observed. No other differences between the shapes seem to exist.

### 4.3. Reliability of the measurement.

There was no precise flow meter available for reference measurements. A simple mechanical flow meter has been used to have a possibility to provide the required water flow approximately and to observe the stability of the flow during the experiment. However, the velocity  $v_F$  measured by the flow meter cannot be used as a reliable reference. Firstly, it measures the flow velocity only locally, in a radial position close to the axis of the pipe. Secondly, in the recent experiment the flow meter was used for flows that were higher than the range for which calibration coefficients were available. The flow was thus estimated by extrapolating the existing calibration coefficients. It seems that the flow meter worked quite well as an indicator of the stability of the water flow. The results are listed in Table 2. A few individual readouts per each measurement and a mean value are given.

Table 2. Results of measurements with the flow meter.

Measure- ment #	$v_{Fi}$ m/s	$v_F = \bar{v}_{Fi}$ m/s	Measure- ment #	$v_{Fi}$ m/s	$v_F = \bar{v}_{Fi}$ m/s
789	0.889	0.887	793	0.879	0.879
	0.892			0.880	
	0.884			0.877	
	0.883		794	0.454	0.454
	0.888			0.452	
790	0.887	0.884	795	0.452	0.453
	0.883			0.453	
	0.882			0.454	
	0.887		796	0.453	0.453
	0.882			0.453	
791	0.879	0.881	797	0.451	0.452
	0.884			0.453	
	0.880			0.453	
792	0.879	0.879	798	0.455	0.455
	0.880			0.454	
	0.878				

Program TD1 was used for elaboration of the recorded time distributions of counts. Results of the peak analysis from all measurements are presented in Table 3. The table

contains a direct output data from the program. Other parameters, such as the channel width and the water flow velocity, are listed in Tables 4 and 5 relevant to a discussion on the influence of various experimental parameters on the final result of the measurement.

**Table 3.** Time distribution analysis from individual measurements.

Measure- ment #	$t_d$ ms	$t_{m0}$ ms	$FWHM_0$ ms	$t_{m1}$ ms	$FWHM_1$ ms	Figure #
789	1400	600	457	1906	483	7a, 7b, 8
790	1400	601	454	1908	480	8
791	1400	629	537	1942	556	9,10a,10b,11
792	1400	627	520	1940	546	10a, 10b, 11
793	1400	635	546	1945	554	10a, 10b, 11
794	2800	1050	1034	3626	1177	12, 13
795	2800	1075	1054	3654	1191	13
796	2800	1054	1005	3638	1199	13, 17a, 17b
797	2800	1081	1040	3674	1249	16, 17a, 17b
798	2800	1088	1041	3674	1240	16, 17a, 17b

*a) Measurements at water flow  $v = v_A$  with  $\Delta t = 50$  ms.*

A certain water flow velocity, close to the maximum possible in the experimental system, was fixed, say  $v = v_A$ , and a readout of the flow meter was also obtained,  $v = v_{FA}$ .

Results of two experiments to measure water flow velocity by pulsed activation are presented in Figs 7 and 8 and in Table 4. Unfortunately, the time channel width used,  $\Delta t = 50$  ms, appeared to be a bad choice. A strange shape of the distribution in Fig.7a is observed.

*Explanation:*

A STARBURST system subroutine, SECNDS(a), is used for the timing purposes in the system. The

accuracy of the value returned by the subroutine is defined as 20 ms. Usually it is much better but just at the period of 50 ms the largest uncertainty happens (not always, this depends on a placement of the call of the subroutine in the program and on the start moment of the task with respect to the computer clock).

In Fig.7b a compression factor was used ( $c = 2$ ) to plot the same data averaged over two channels. A much smoother curve is the result, which means that the deviations were really spread regularly. Note that the original data are always used in the procedure of the peak analysis (see pictures at corners of the plots in Figs 7a and 7b).

Results of the two measurements are compared in Fig.8 and in Table 4. They agree excellent in spite of the problem of the channel width.

*b) Measurements at water flow  $v = v_A$  with  $\Delta t = 40$  ms.*

For the next series of experiments the time channel width was changed to the minimum possible value assumed in the system,  $\Delta t = 40$  ms, when the relative inaccuracy of the channel width can reach 50%. The result of experiment #791 looks much better than that of experiment #790 – see Fig.9 where  $c = 1$ . In other experiments, however, small errors of the mentioned type have been observed although they never reached the level observed while using 50 ms channels. The time distributions of the pulses from detector #0 in three experiments repeated under identical circumstances (the same  $\Delta t$ , the same  $v$ ) are shown in Fig.10a and from detector #1 – in Fig.10b. A perfect consistency is visible when the data are smoothed (see Fig.11,  $c = 2$ ). The flow velocities obtained are listed in Table 4.

**Table 4.** Water flow velocities ( $v=v_A$ ) measured by the neutron method and by a flow meter.

Measure- ment #	$\Delta t$ ms	$v_{01A}$ cm/s	$v_{FA}$ cm/s	$\frac{v_{01A}}{v_{FA}}$
789	50	73.12	88.7	0.824
790	50	73.07	88.4	0.827
791	40	72.73	88.1	0.826
792	40	72.73	87.9	0.827
793	40	72.90	87.9	0.829

c) *Measurements at water flow  $v = v_B$  with  $\Delta t = 40$  ms.*

Three experiments were made at the water flow velocity  $v = v_B \approx 0.5 v_A$  which was adjusted by means of the flow meter. The same channel width was used for a direct accurate comparison with the experiments made with  $v = v_A$ . One of the results is shown in detail in Fig.12. The reason for certain irregularities observed in the shape of the peaks is the same as explained above in Case a.

A very good reproducibility of the measurements is demonstrated in Fig.13 and in Table 5.

A comparison of the peak shapes obtained from detector #0 at the two different velocities,  $v_A$  and  $v_B$ , is given in Fig.14. Two full distributions (from both detectors) obtained at the different water flow velocities are plotted in the same time scale in Fig.15 and show the peak propagation.

d) *Measurements at water flow  $v = v_B$  with  $\Delta t = 60$  ms.*

Two experiments were made when the water flow velocity was kept the same and the multiscaler channel width was changed to  $\Delta t = 60$  ms. The reproducibility of the two measurements, experiments #797 and #798, is shown in Fig.16. The results are given in Table 5.

Table 5. Water flow velocities ( $v=v_B$ ) measured by the neutron method and by a flow meter.

Measure- ment #	$\Delta t$ ms	$v_{01B}$ cm/s	$v_{FB}$ cm/s	$\frac{v_{01B}}{v_{FB}}$
794	40	37.07	45.3	0.818
795	40	37.03	45.3	0.817
796	40	36.96	45.3	0.816
797	60	36.83	45.2	0.815
798	60	36.93	45.5	0.812

A comparison of these results with the measurements done with  $\Delta t = 40$  ms is presented in Figs 17a and 17b. The numbers of channels plotted were chosen to get precisely the same time interval and scale ( $126 \times 40$  ms =  $84 \times 60$  ms = 5040 ms). In Fig.17a individual points are marked and the y-scale is the same for both plots. In Fig.17b the y-scales are normalized by the ratio of the channel widths.

From the data given in Tables 4 and 5 an experimental relation between the two water velocities,  $v_B$  and  $v_A$ , has been found:

$$\bar{v}_{01B} = 0.507 \bar{v}_{01A} \quad (\text{neutron experiments}),$$

$$\bar{v}_{FB} = 0.514 \bar{v}_{FA} \quad (\text{flow meter measurements in the same experiments}),$$

which means that the relative dependence between the two different water flow velocities has been found to be the same from the neutron measurement and from the flow meter readout in spite of the existing differences in absolute values.

## 5. Conclusions.

The experiments performed show a high reproducibility of the measurements and a high reliability in detection of a change of the water flow velocity. The two  $\gamma$  detectors method is recommended. The precision of the measurement can be farther improved by preparing a more advanced and dedicated measurement setup and by using a more advanced analysis of the time distributions of counts. The incident neutron beam should be collimated to avoid the irradiation of a too thick layer of the flowing water. Collimators should be also used at the detector openings. A higher timing precision of the multiscaler has to be used than was possible in this preliminary experiment. The correlation method can be used for treatment of the collected data and a consideration of the peak shape can be included (the influence of the radioactivity decay in time, of the diffusion of molecules, of the water velocity profile).

A big advantage of the method is that the measuring equipment is placed outside a pipe and no technical changes are needed in an existing piping system where the water flow is to be measured. The activation intensity and the distances between the neutron generator and detectors can be easily adjusted to a local geometry and to the water flow velocity range.

## Acknowledgements

The idea of the experiment comes from Prof. Imre Pázsit and Dr. Gudmar Grosshög. Engs. Rickard Rydz, Lennart Norberg and Lasse Urholm, gave technical help at the creation of the experimental setup. M.Sc. Andrzej Igielski (Inst. of Nuclear Physics, Kraków, Poland) participated in some parts of the experiment.

## References

- ALIEV A.I., DRYNKIN V.I. and LEIPUNSKAYA V.A. (1970)  
*Handbook of Nuclear Data for Neutron Activation Analysis.*  
IPST, pp. 23, 47.
- BARRET P.R. (1982)  
An Examination of the Pulsed-Neutron Activation Technique for Fluid Flow Measurements.  
Nucl. Eng. Des. 74, 183-192.
- SCOTT H.D., PEARSON C.M., RENKE S.M., MCKEON D.C. and MEISENHEDER J.P. (1993)  
Applications of Oxygen Activation for Injection and Production Profiling in the Kuparuk River Field.  
SPE Formation Evaluation 8, 103-111.
- ZUBER A. (1986)  
Tracer Experiments in Variable Flow.  
Appl. Radiat. Isot. 37, 1077 (Int.J.Radiat.Appl.Instrum. A).



## List of figures.

Fig.1. Geometry of the measurement.

Fig.2. Instrumentation system for the experiment.

Fig.3. Comparison of the time distributions when two different neutron-activation pulses,  $T_n$ , have been used. The neutron pulse is observed at  $t=1000$  ms.  $N_R$  – number of runs.

Fig.4. Experiment with two detectors in different positions.  $\Delta t = 100$  ms. The delay is given at the middle of the header ( $t_d = -1000$  ms).

Fig.5. Experiment in better conditions for an observation of peaks of the time distributions,  $\Delta t = 50$  ms,  $t_d = 1400$  ms.

Fig.6. Comparison of shapes of peaks of the distributions from detector #0 (closer) and detector #1 (further from the activation point).

Fig.7a. Experiment #798 for a reproducibility test.

Fig.7b. The same data as in Fig.7a plotted with a compression factor  $c = 2$ .

Fig.8. Comparison of the time distributions in two measurements ( $\Delta t = 50$  ms,  $c = 2$ ).

Fig.9. Experiment with a changed time channel width,  $\Delta t = 40$  ms.

Fig.10a. Stability of the F0 peak position.

Fig.10b. Stability of the F1 peak position.

Fig.11. Example of a reproducibility of the measurement ( $c = 2$ ).

Fig.12. Experiment at lower velocity of the water flow,  $v = v_B \approx 0.5v_A$ .

Fig.13. Reproducibility of the experiments at the water flow  $v = v_B$ .

Fig.14. Peak shapes at two different water flow velocities,  $v_B \approx 0.5v_A$ .

Fig.15. Comparison of the peak propagations at two different water flow velocities,  $v_B \approx 0.5v_A$ .

Fig.16. Stability of the measurements with  $\Delta t = 60$  ms at the water flow  $v = v_B$ .

Fig.17a. Comparison of the measurements using  $\Delta t = 40$  ms and  $\Delta t = 60$  ms. The plotted time range is  $t = 2800$  ms +  $[0 \div 5400]$  ms.

Fig.17b. The same comparison as in Fig.17a with the count axis normalized by the ratio of the channel widths.

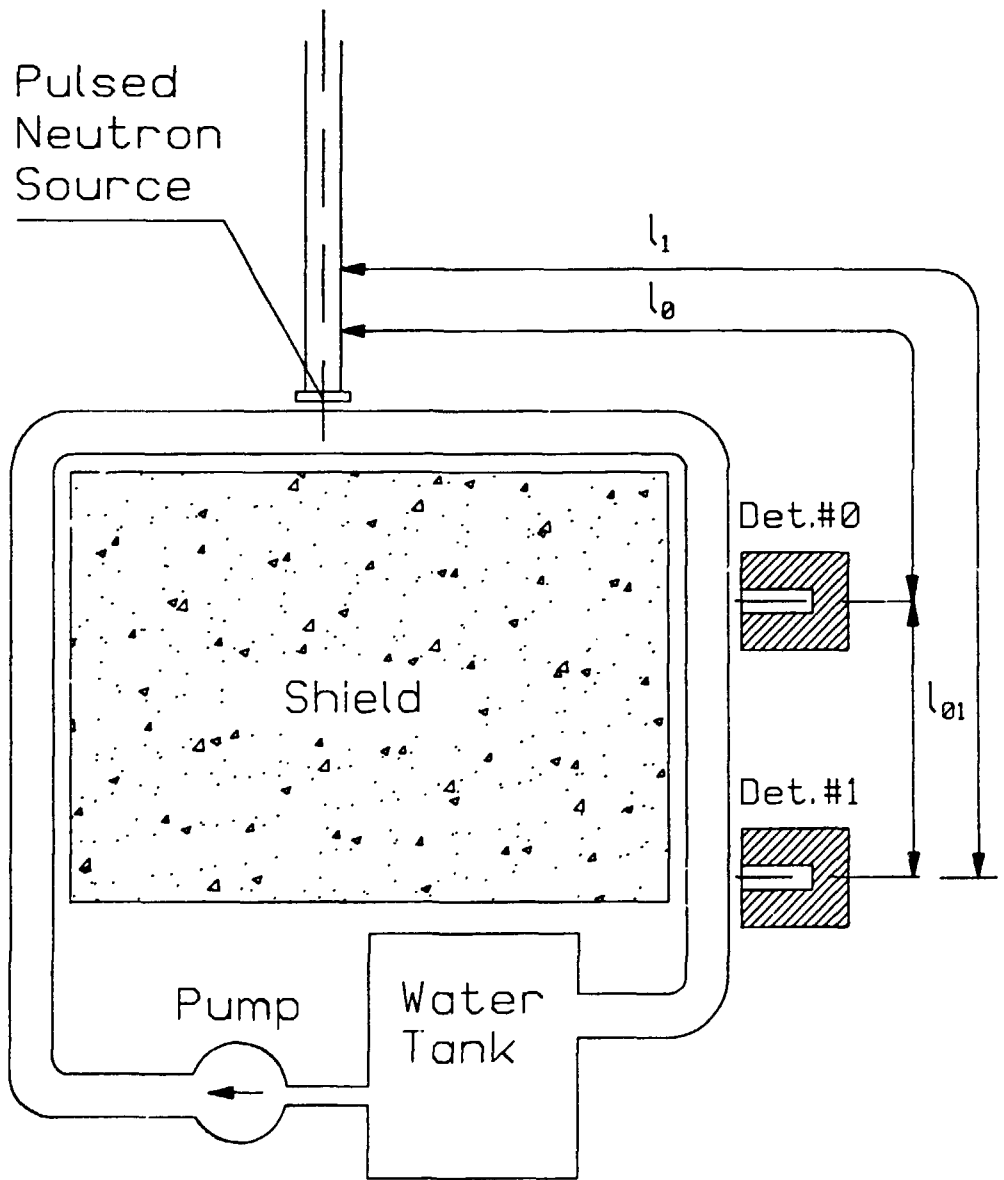


Fig.1. Geometry of the measurement.

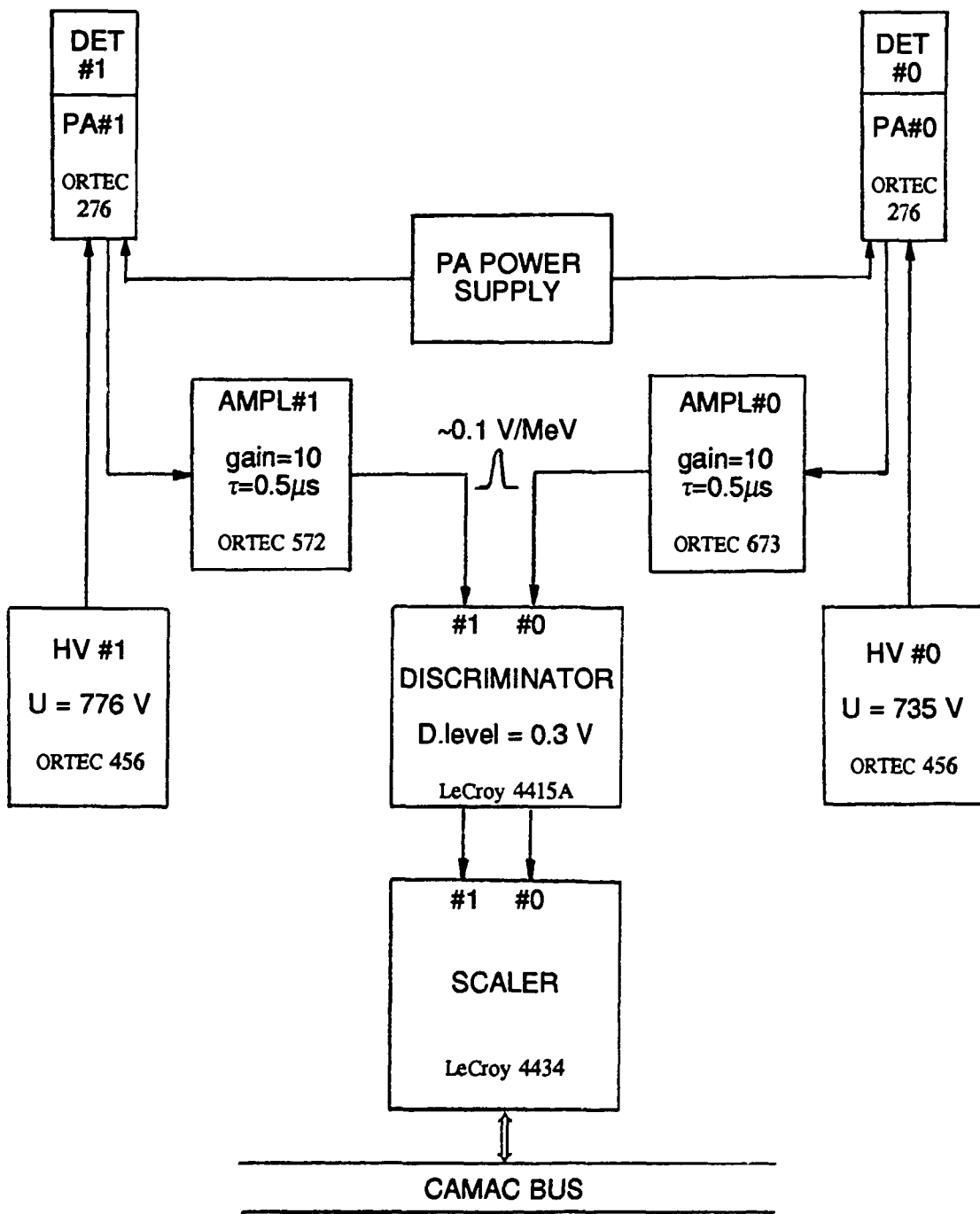


Fig.2. Instrumentation system for the experiment.

DET – detector, PA – preamplifier, AMPL – amplifier, HV – high voltage supply.

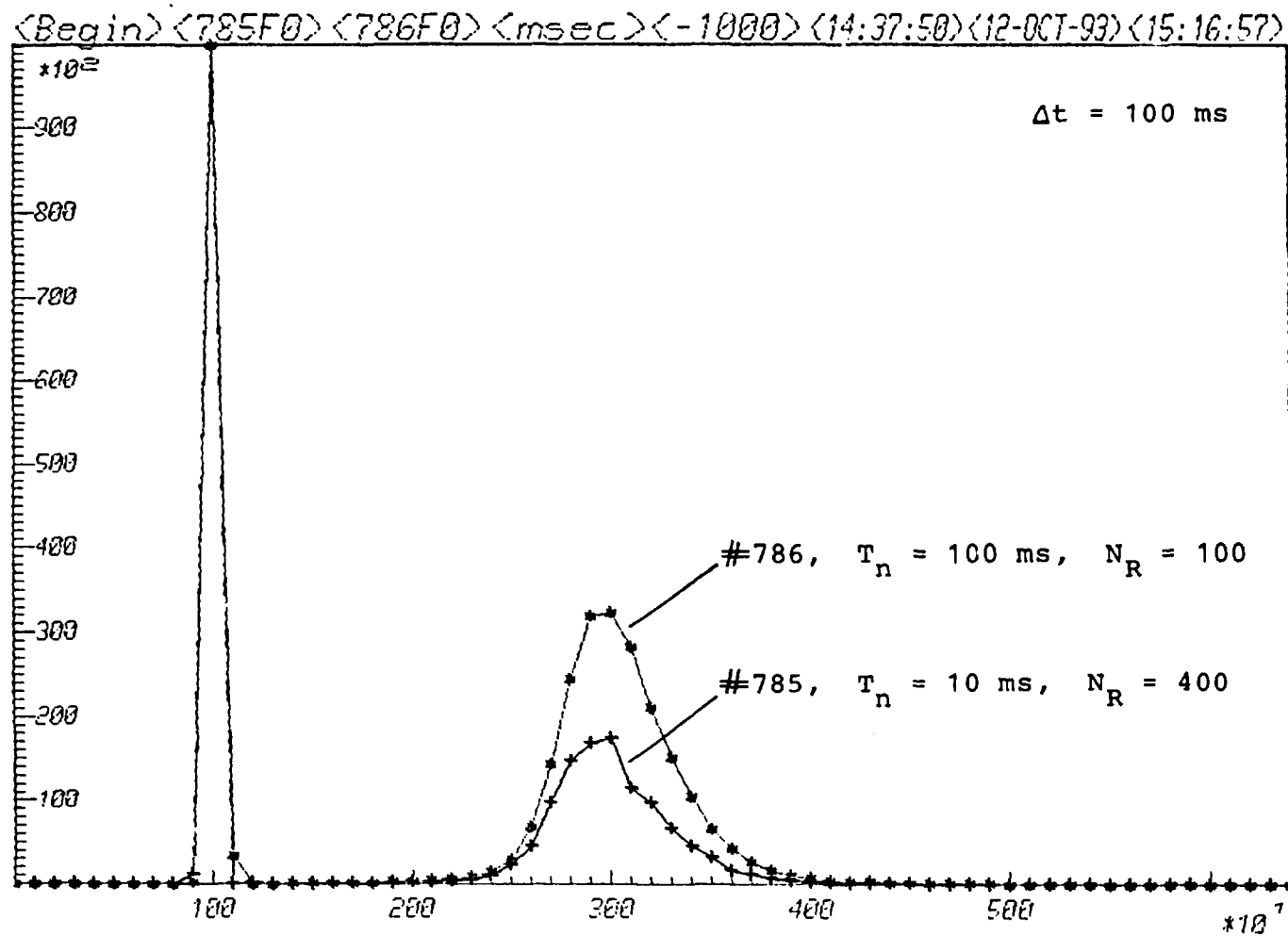


Fig.3. Comparison of the time distributions when two different neutron-activation pulses,  $T_n$ , have been used. The neutron pulse is observed at  $t=1000 \text{ ms}$ .  $N_R$  – number of runs.

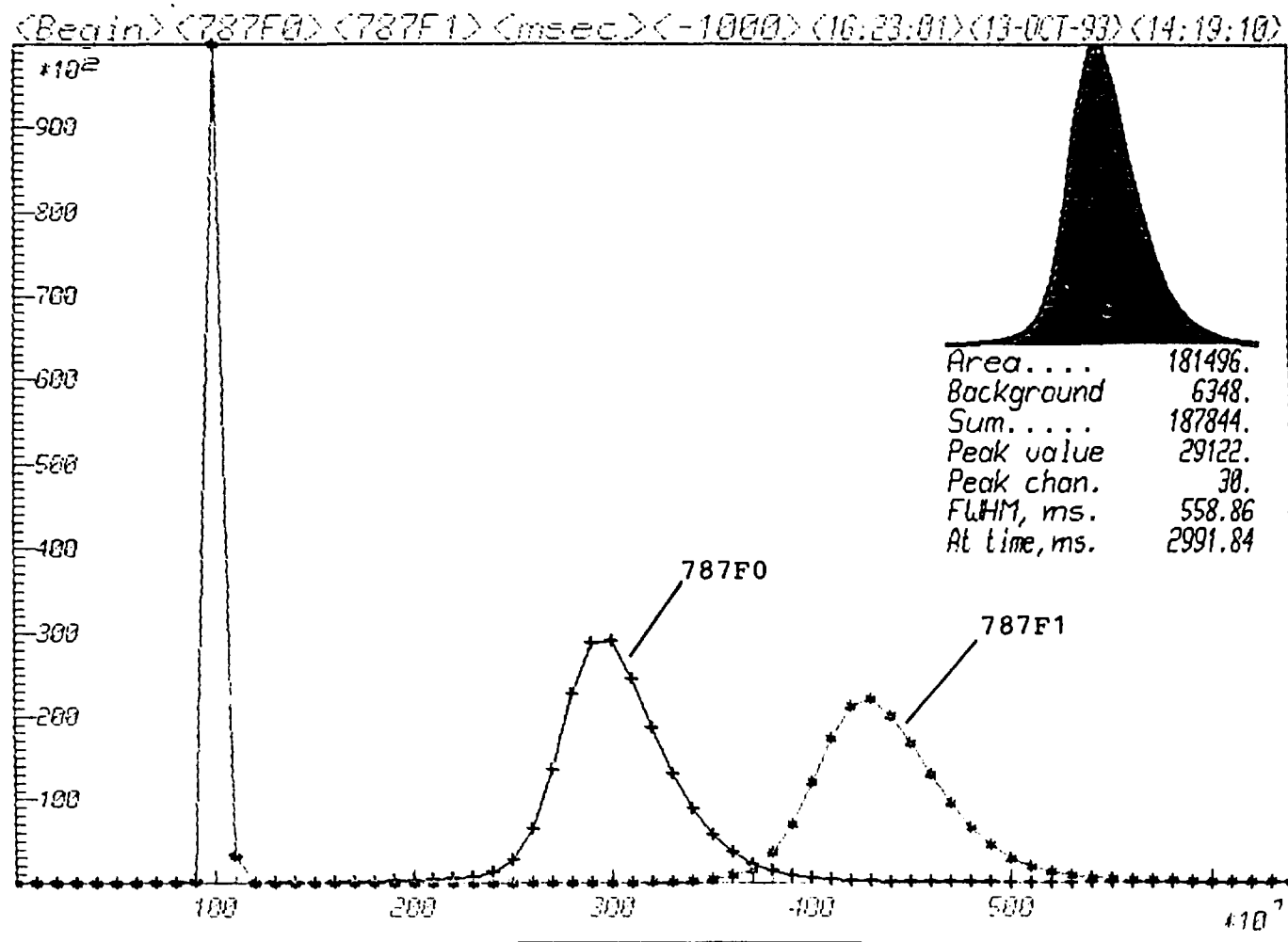


Fig.4. Experiment with two detectors in different positions.  $\Delta t = 100$  ms. The delay is given at the middle of the header ( $t_d = -1000$  ms).

<Begin><788F0><788F1><msec><1400><16:08:08><13-OCT-93><15:46:19>

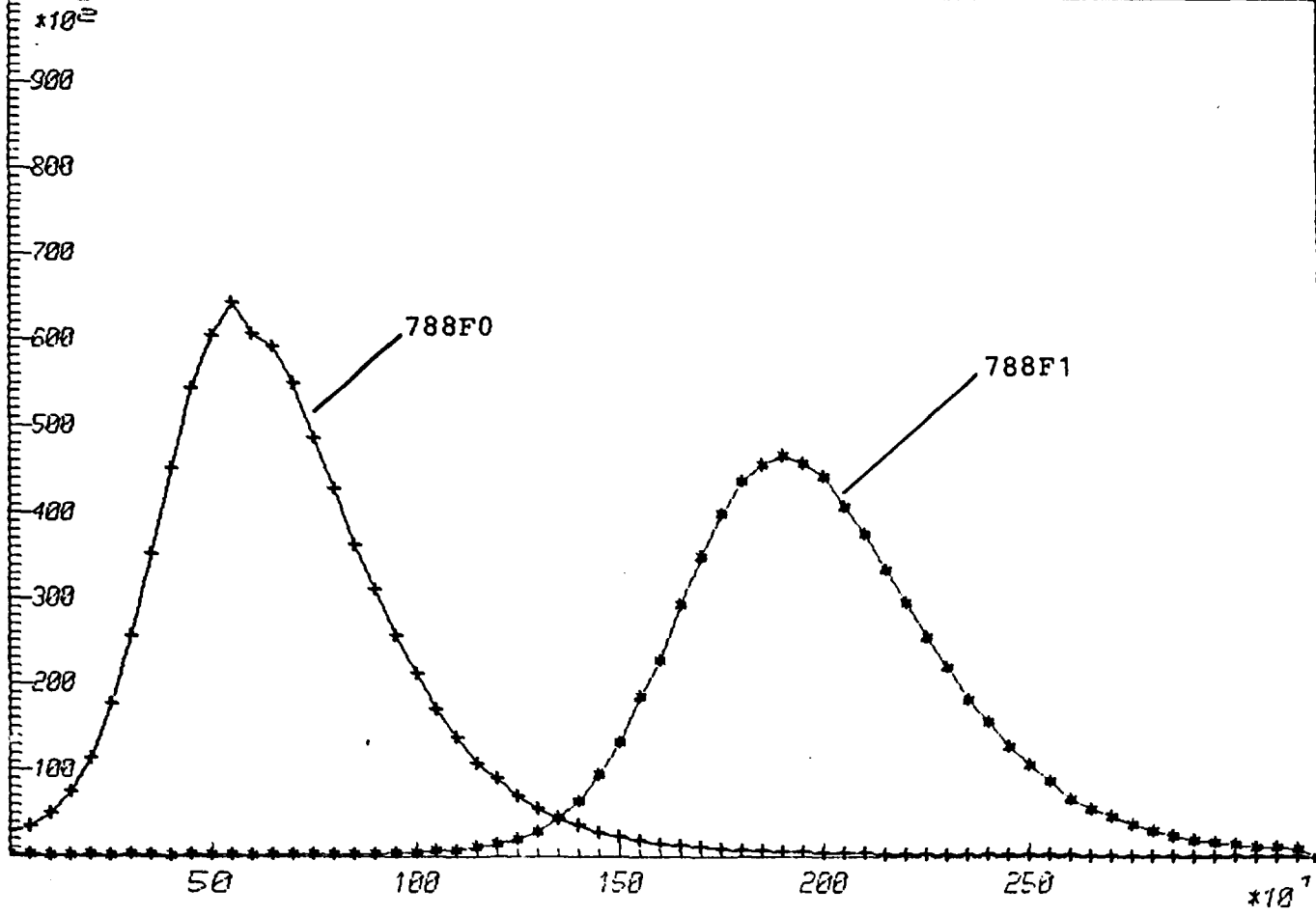


Fig.5. Experiment in better conditions for an observation of peaks of the time distributions,  $\Delta t = 50$  ms,  $t_d = 1400$  ms.

<Begin> <788F0> <788F1> <msec> <1400> <16:04:59> <13-OCT-93> <15:46:19>

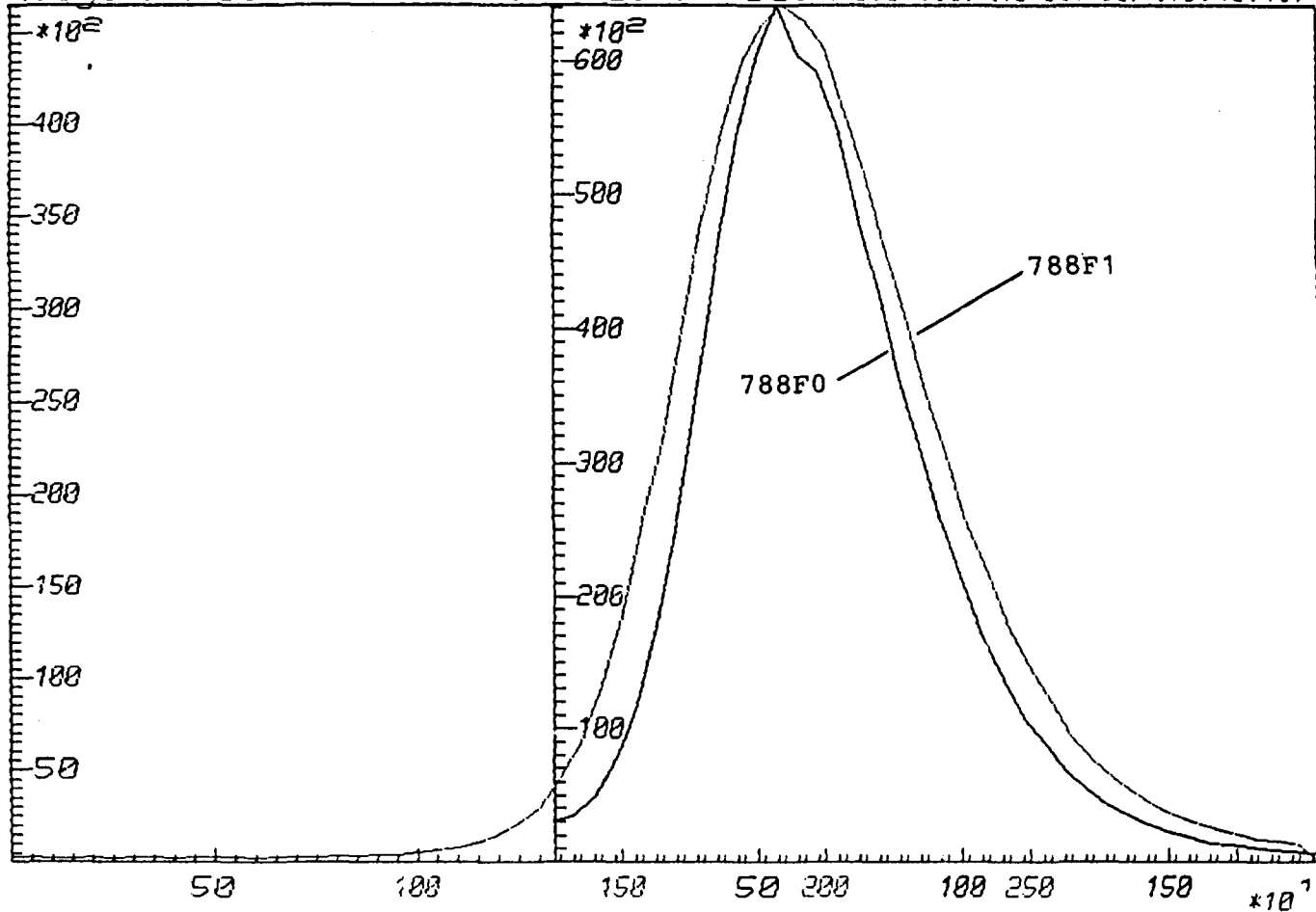


Fig.6. Comparison of shapes of peaks of the distributions from detector #0 (closer) and detector #1 (further from the activation point).

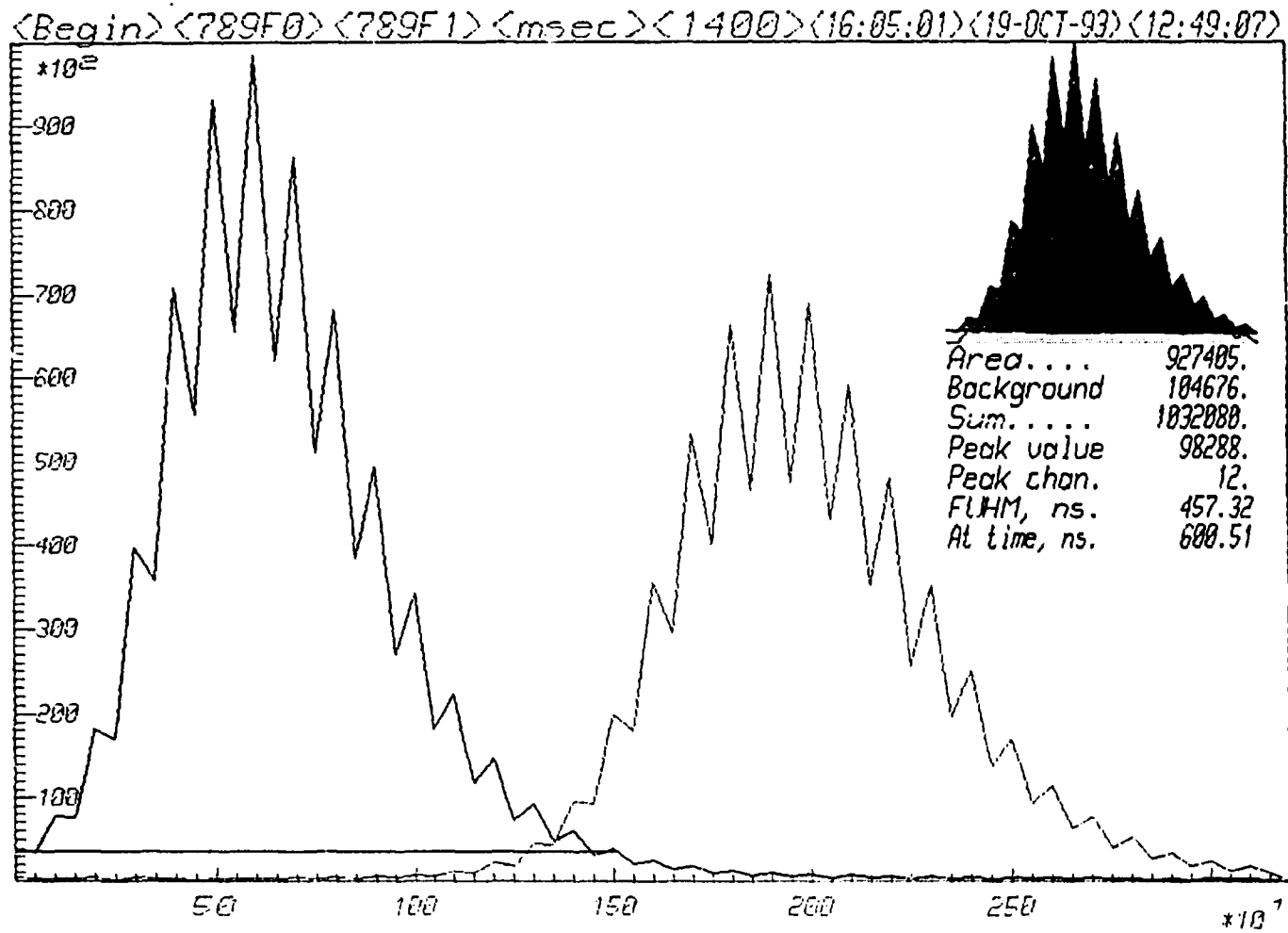


Fig.7a. Experiment #798 for a reproducibility test.

An explanation of the strange shapes is given in the text.



<Begin> <789F0> <789F1> <msec> <1400> <16:00:31> <19-OCT-93> <12:49:07>

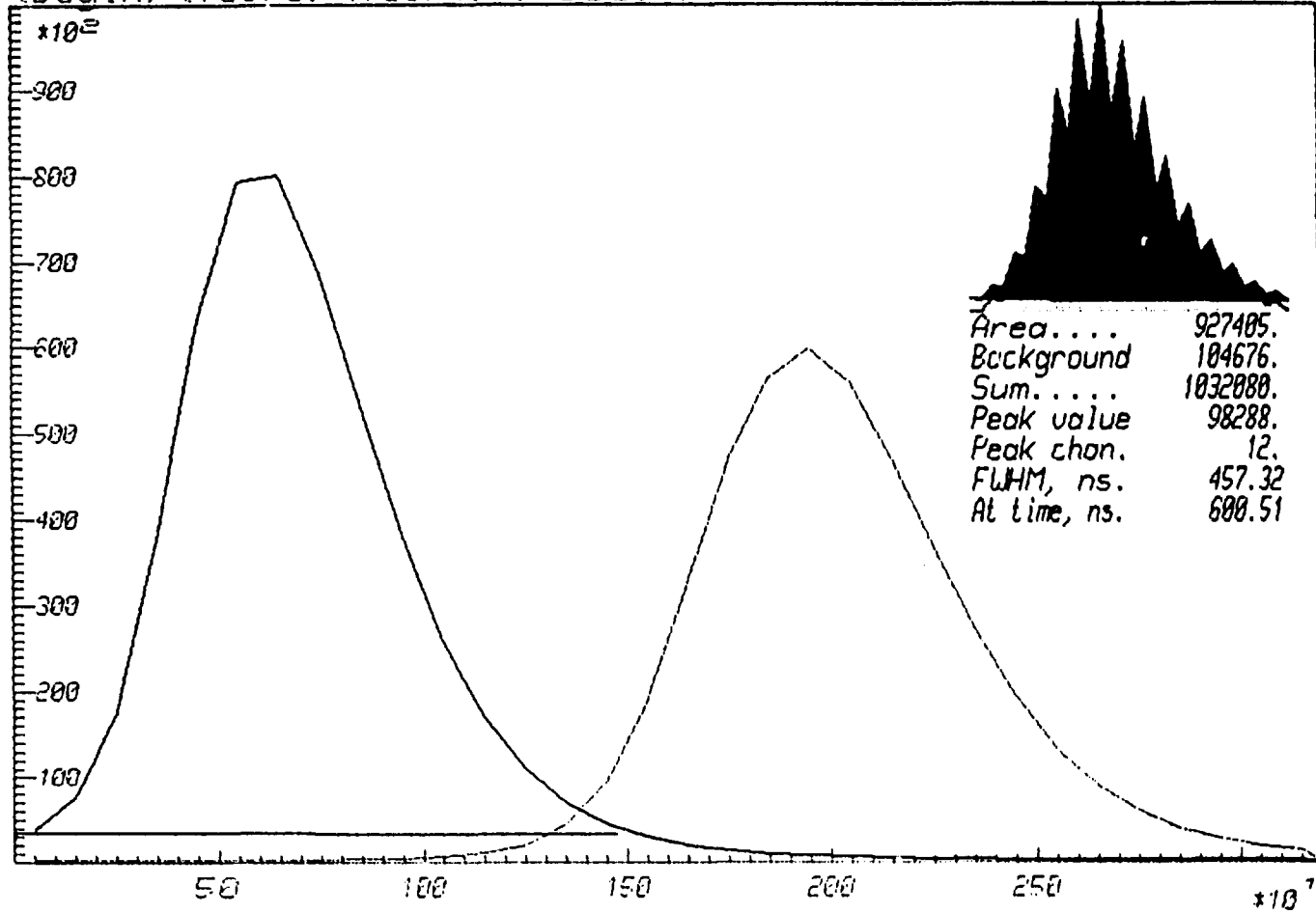


Fig.7b. The same data as in Fig.7a plotted with a compression factor  $c = 2$ .

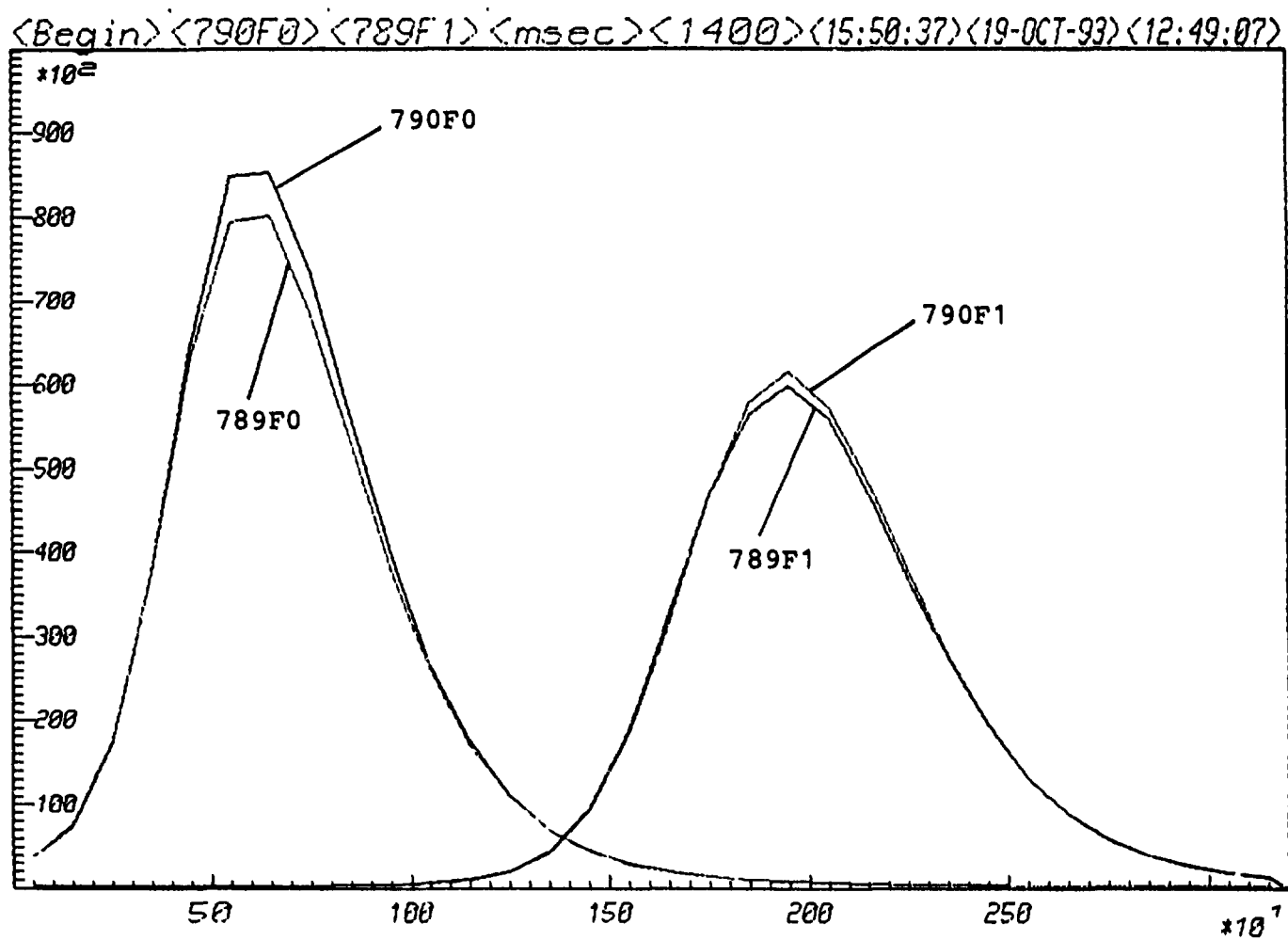


Fig.8. Comparison of the time distributions in two measurements ( $\Delta t = 50$  ms,  $c = 2$ ).

<Begin><791F0><791F1><msec><1400><09:51:22><19-OCT-93><13:11:51>

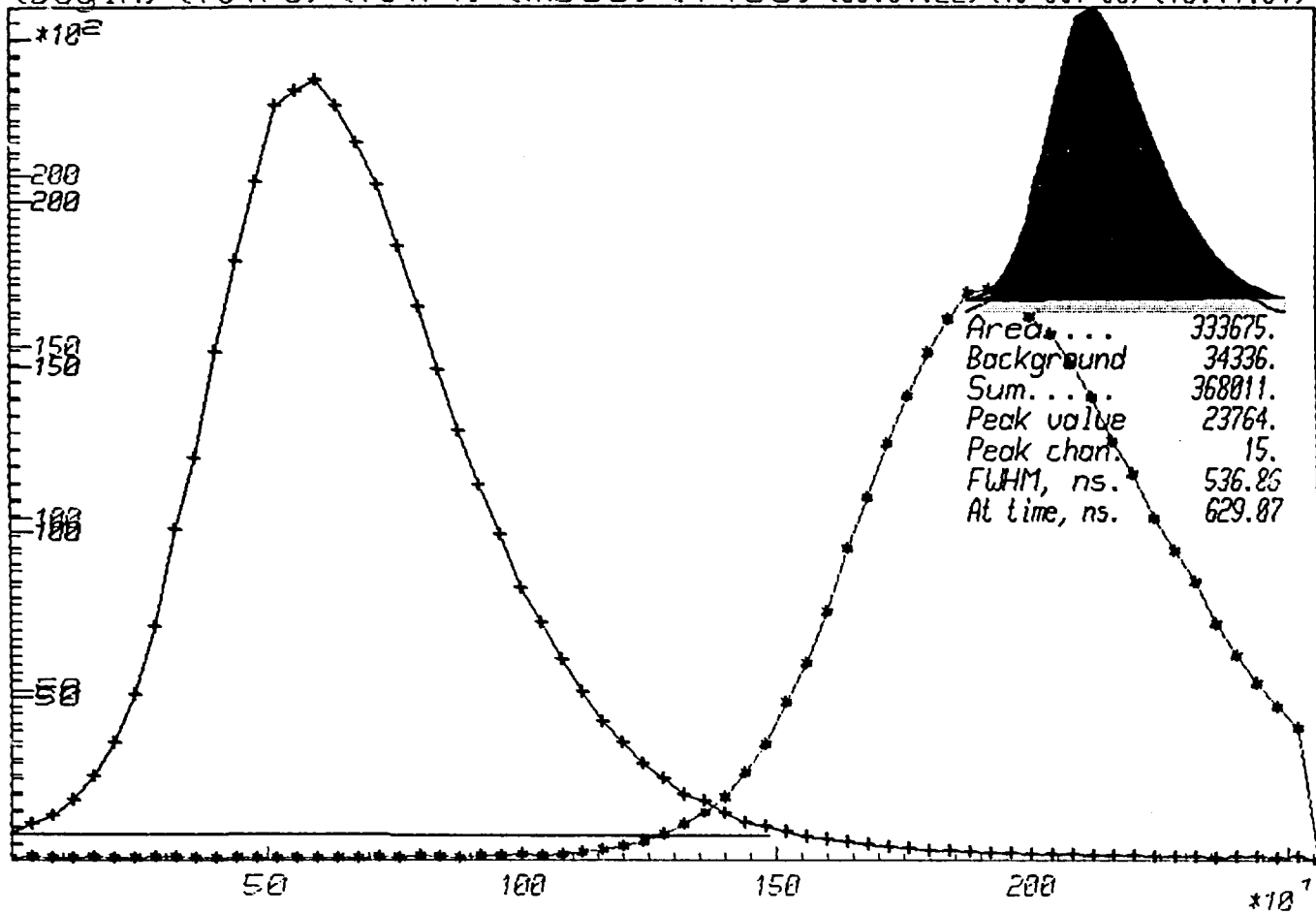


Fig.9. Experiment with a changed time channel width,  $\Delta t = 40$  ms.

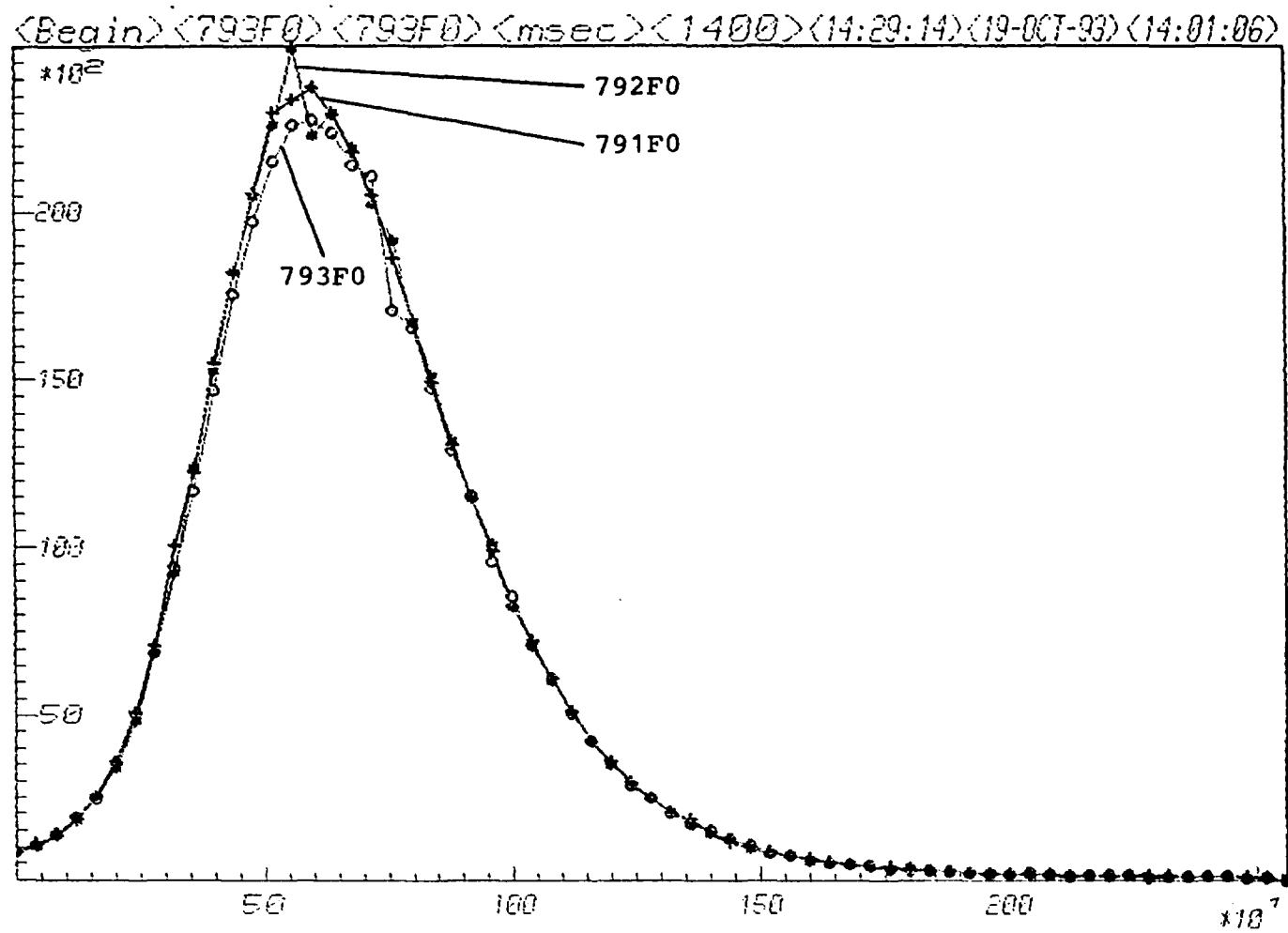


Fig.10a. Stability of the F0 peak position.

<Begin> <793F0> <793F1> <msec> <1400> <14:33:54> <19-OCT-93> <14:01:06>

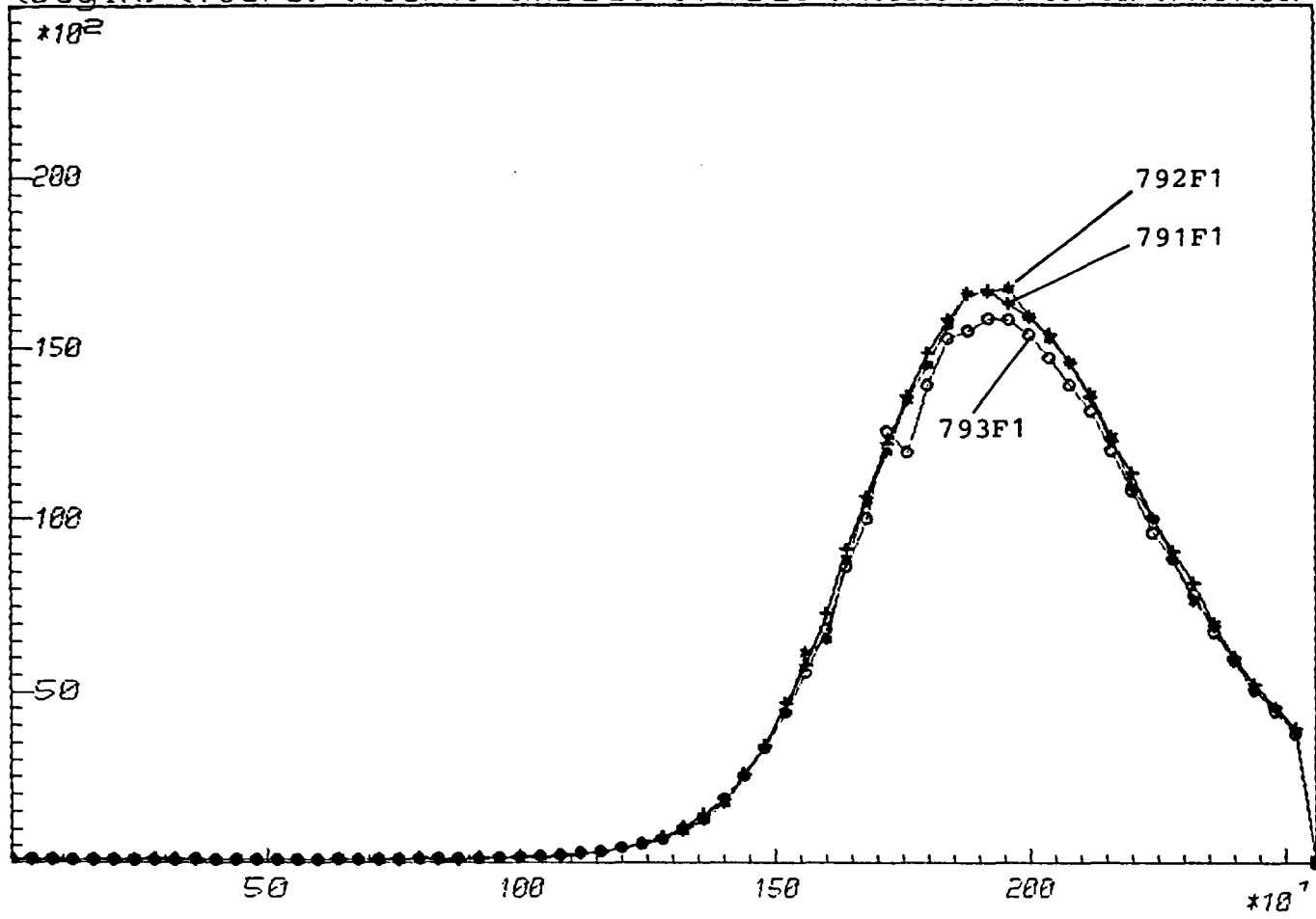


Fig.10b. Stability of the F1 peak position.

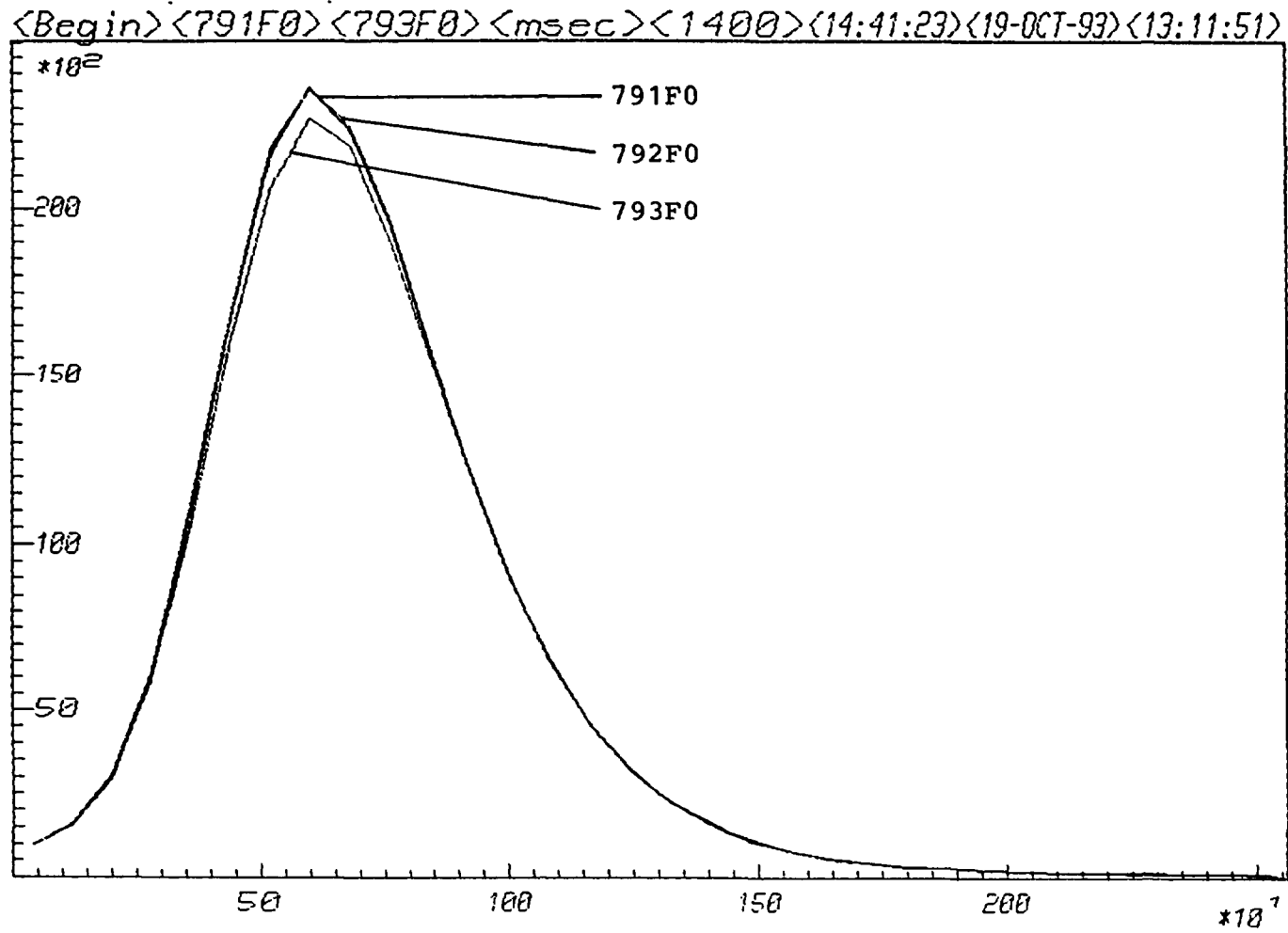


Fig.11. Example of a reproducibility of the measurement ( $c = 2$ ).

<Begin> <794F0> <794F1> <msec> <2800> <16:33:05> <20-OCT-93> <10:14:56>

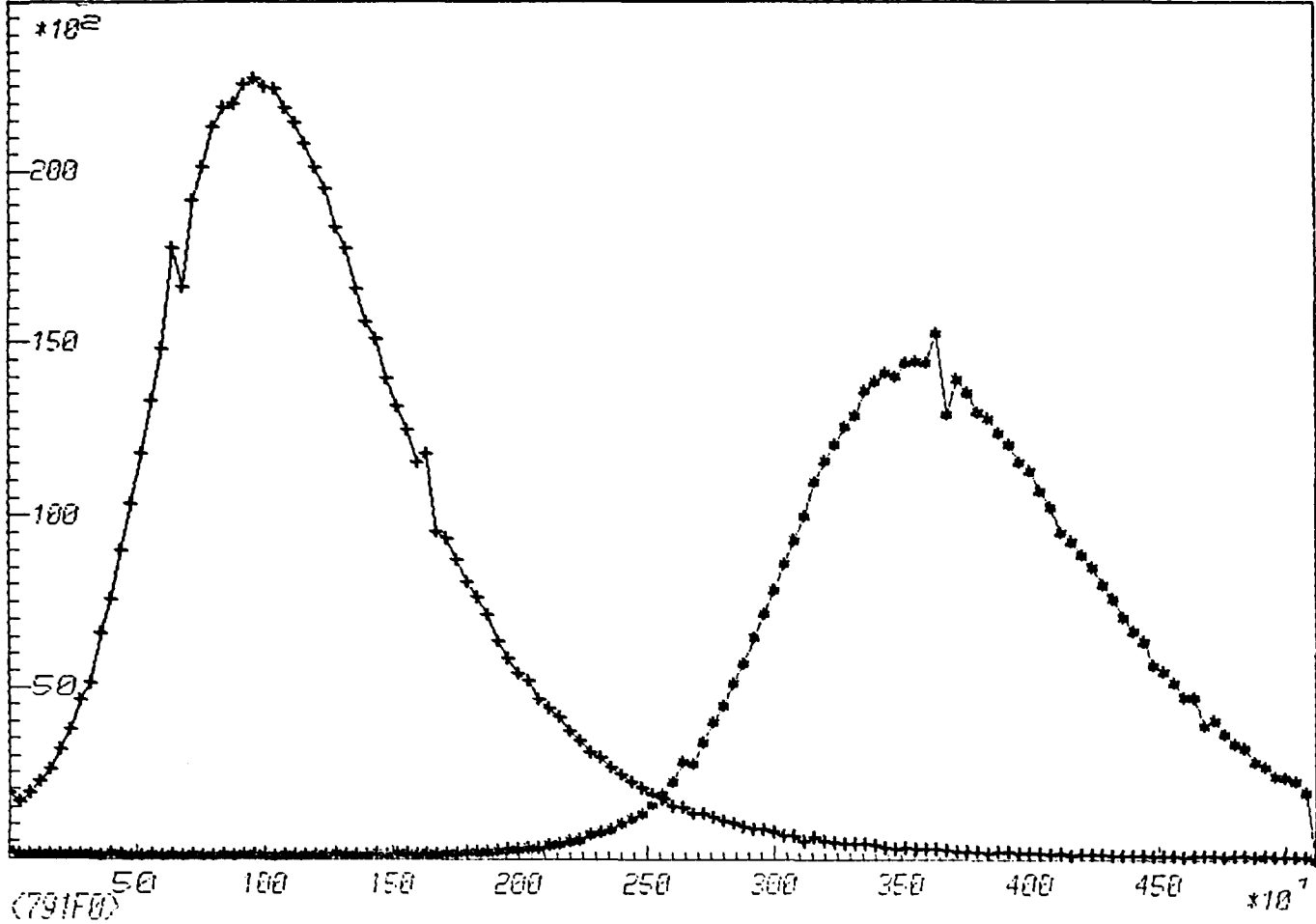


Fig.12. Experiment at lower velocity of the water flow,  $v = v_B \approx 0.5v_A$ .

(Note the multiscaler delay and range being twice longer than at  $v = v_A$ ).

<Begin> <794F0> <796F1> <msec> <2800> <17:37:24> <20-OCT-93> <10:14:56>

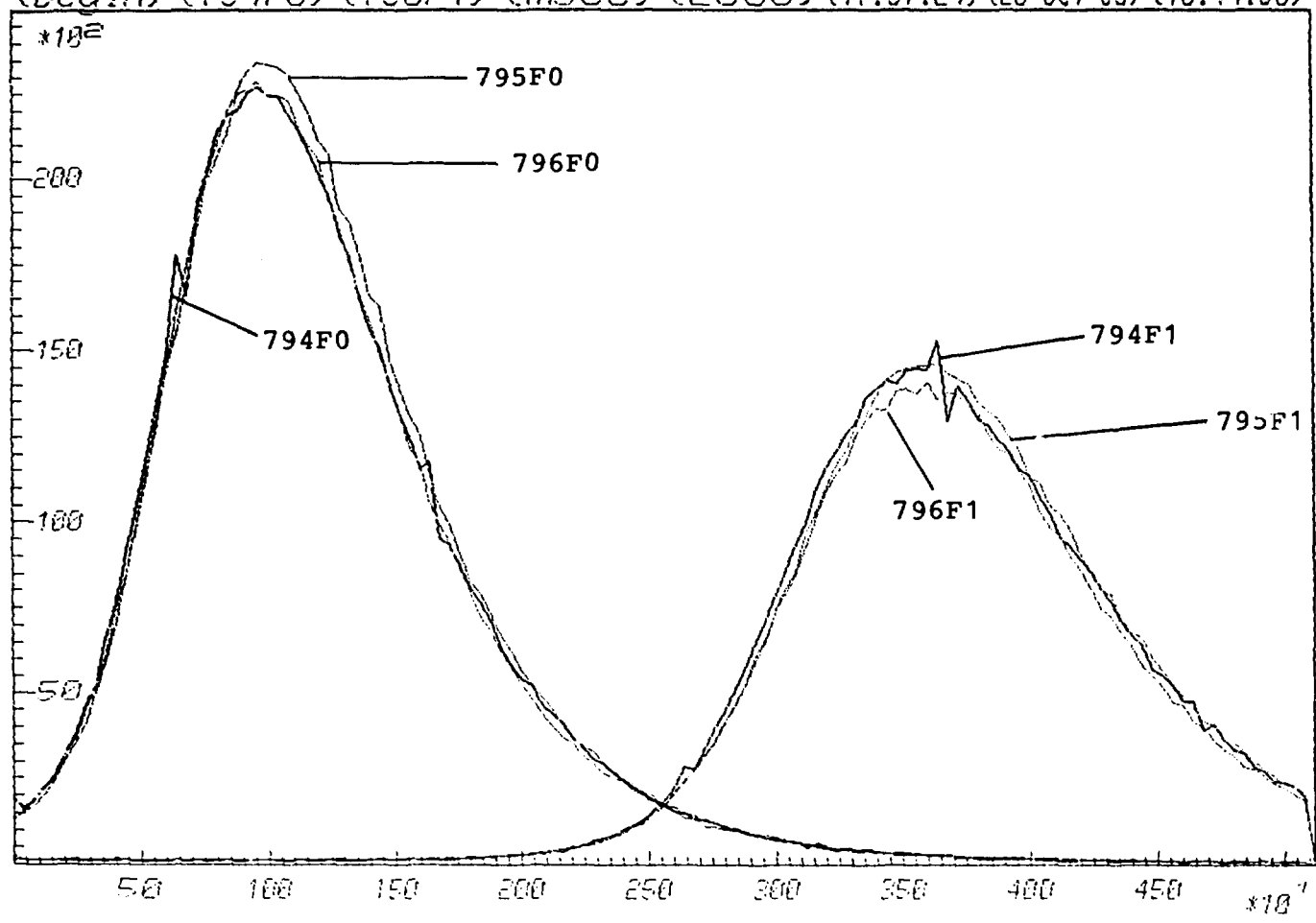
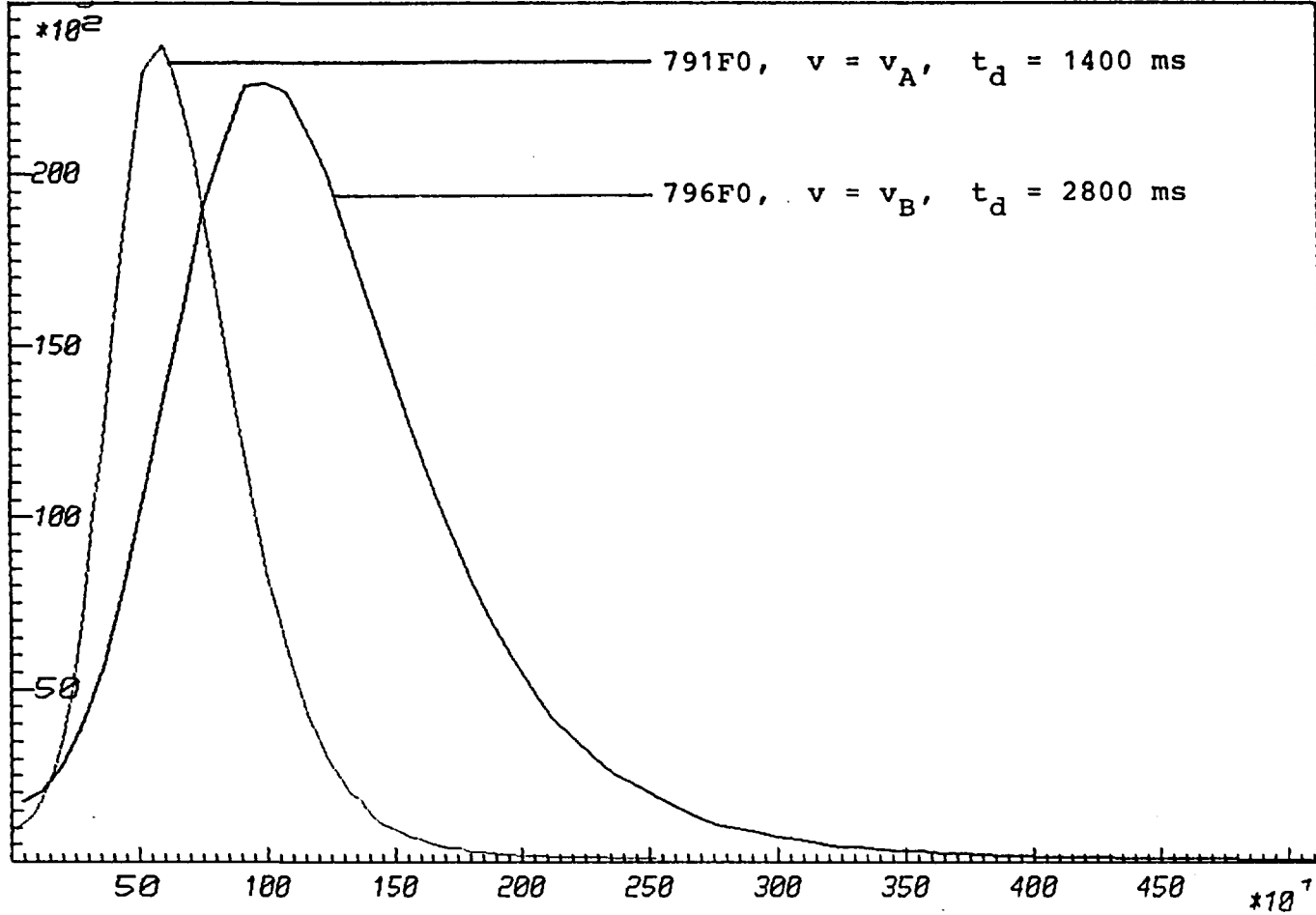


Fig.13. Reproducibility of the experiments at the water flow  $v = v_B$ .



<Begin> <796F0> <791F1> <msec> <2800> <10:15:17> <20-OCT-93> <11:20:11>



33

Fig.14. Peak shape at two different water flow velocities,  $v_B \approx 0.5v_A$ .

<Begin> <796F0> <791F1> <msec> <2800> <10:29:19> <20-OCT-93> <11:20:11>

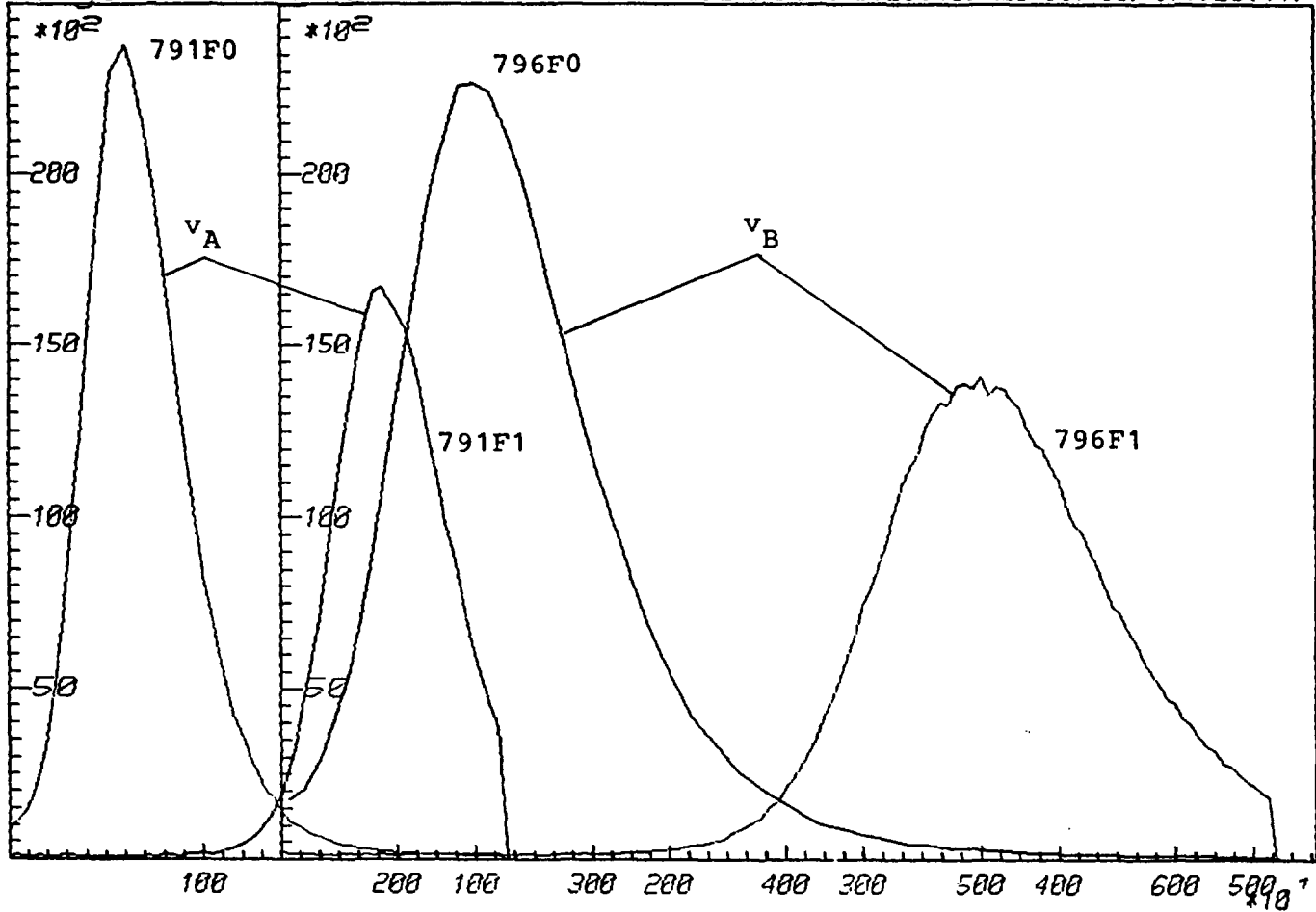


Fig.15. Comparison of the peak propagations at two different water flow velocities,  
 $v_B \approx 0.5v_A$ .

<Begin><797F0><798F1><msec><2800><10:04:48><20-OCT-93><12:05:53>

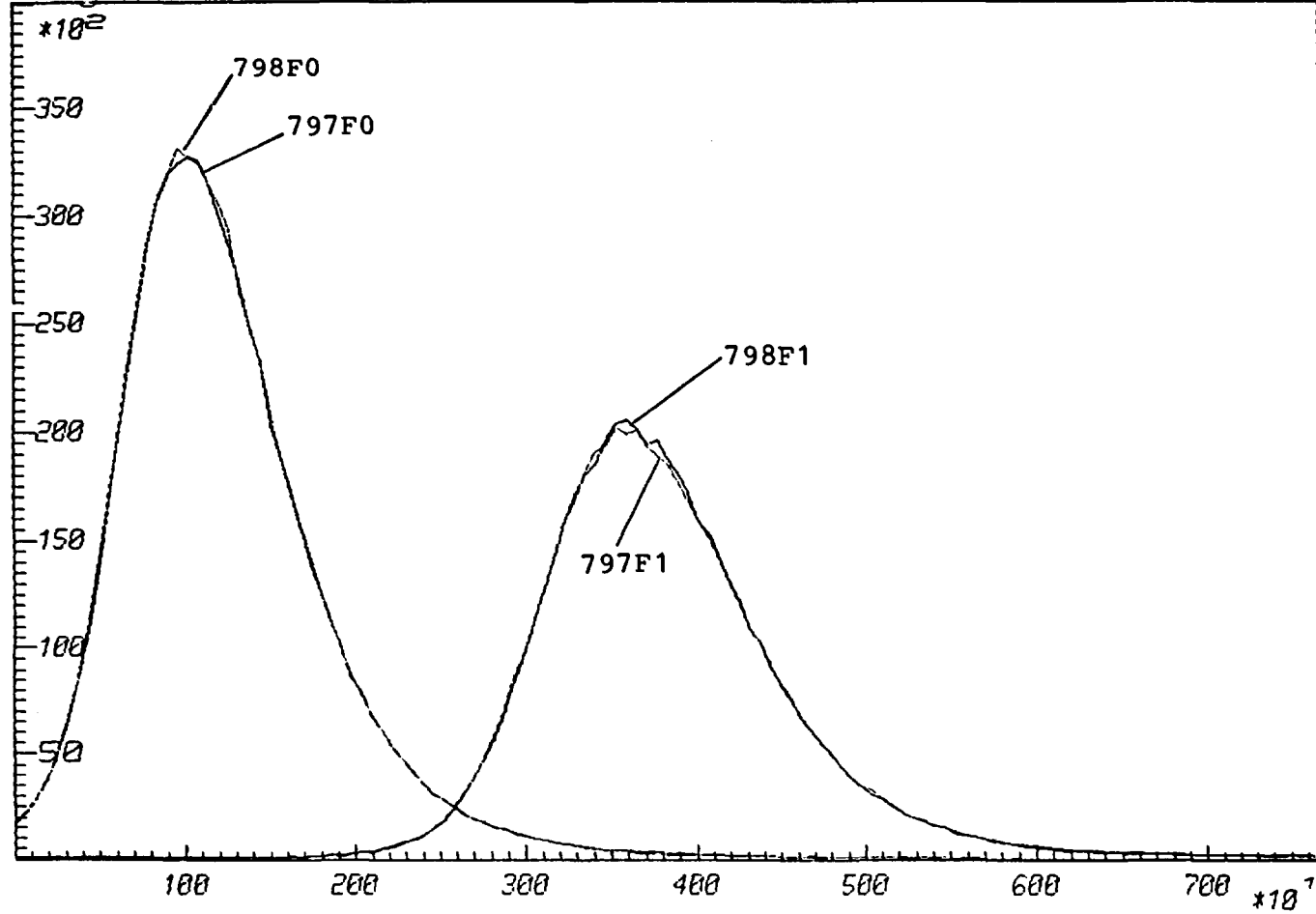


Fig.16. Stability of the measurements with  $\Delta t = 60$  ms at the water flow  $v = v_B$ .

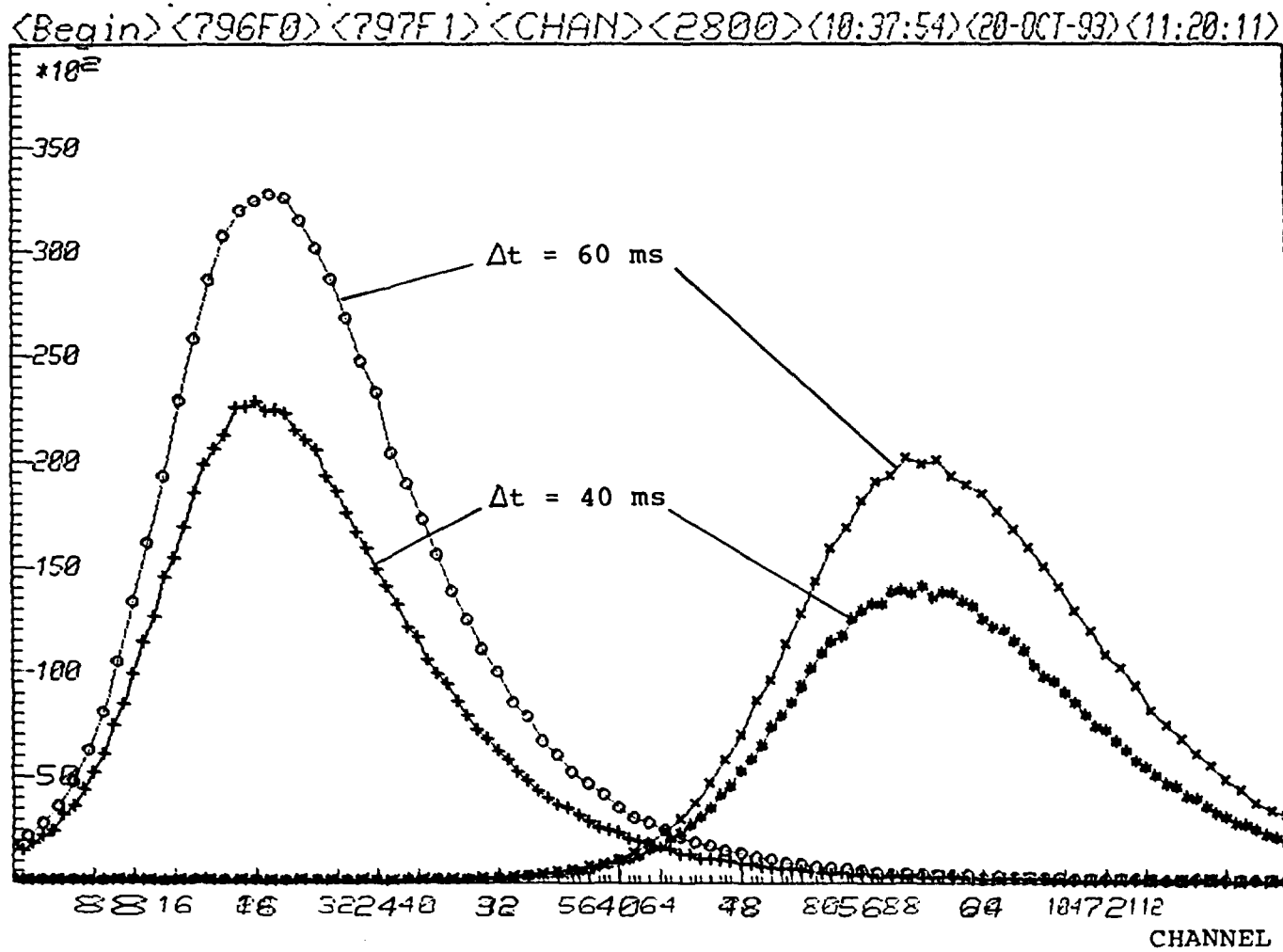


Fig.17a. Comparison of the measurements using  $\Delta t = 40$  ms and  $\Delta t = 60$  ms. The plotted time range is  $t = 2800$  ms +  $[0 \div 5400]$  ms.

<Begin> <796F0> <797F1> <CHAN> <2800> <10:48:45> <20-OCT-93> <11:20:11>

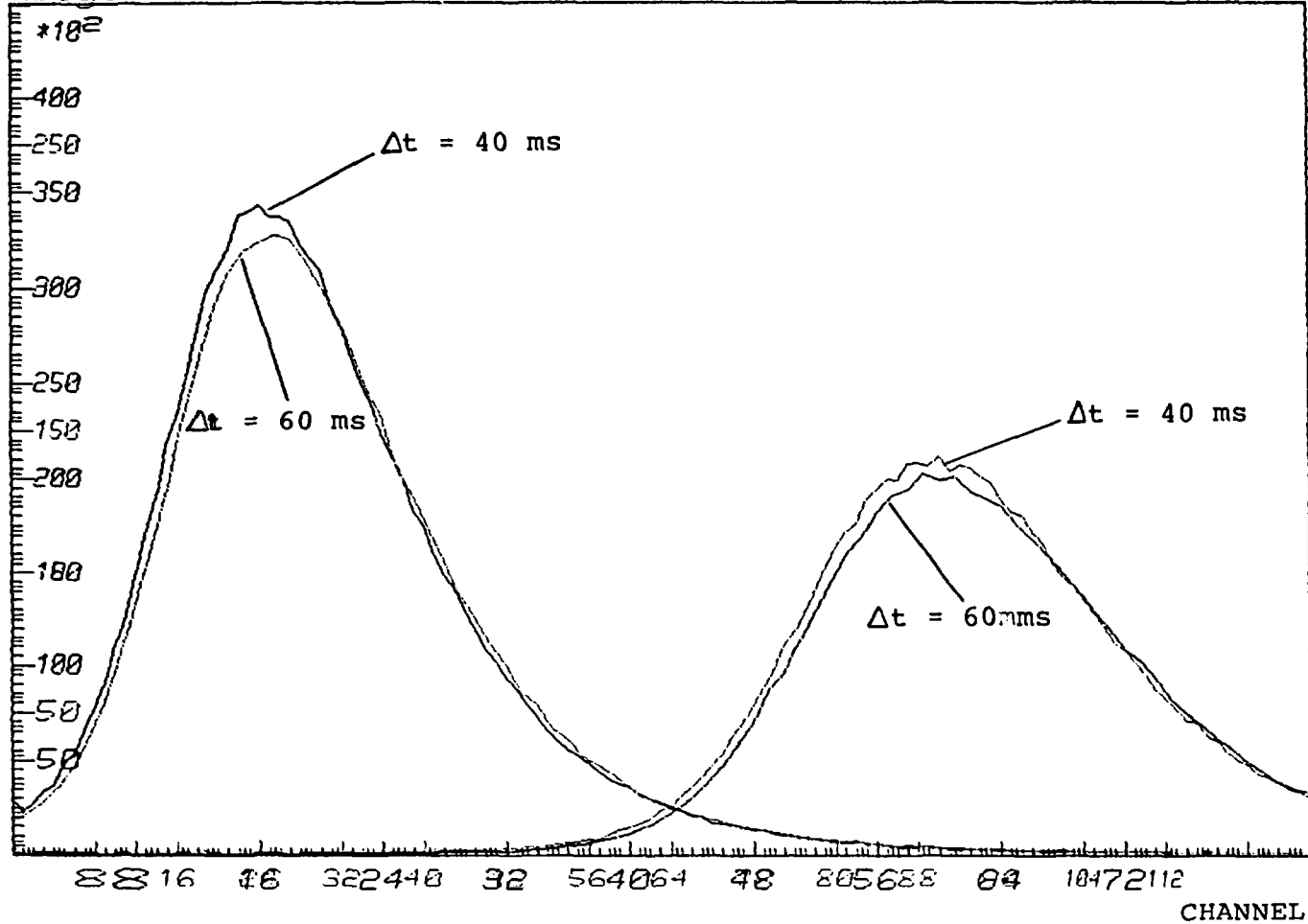


Fig.17b. The same comparison as in Fig.17a with the count axis normalized by the ratio of the channel widths.

## APPENDIX A

### Documentation of the experiments.

The data are stored in directory DU1:[6,2] of the STARBURST CES computer. The experimental conditions are listed in files 784F0.LOG to 798F0.LOG . The TD1 parameters are saved in the corresponding files 784F0.T1P to 798F0.T1P . The experimental data (the time distributions given by a contents of channels) are stored in files 784F0.T1D to 798F0.T1D for detector #0, and in 787F1.T1D to 798F1.T1D for detector #1.

#### A.1. List of the experimental conditions in individual measurements.

```
784 ; experiment name
  0 ; max. Line#
  0 ; delay (msec)
 100 ; channel width
  64 ; number of channels used
  10 ; neutron pulse repetition (sec)
 400 ; number of runs
```

```
785 ; experiment name
  0 ; max. Line#
-1000 ; delay (msec)
 100 ; channel width
  64 ; number of channels used
  10 ; neutron pulse repetition (sec)
 400 ; number of runs
```

```
786 ; experiment name
  0 ; max. Line#
-1000 ; delay (msec)
 100 ; channel width
  64 ; number of channels used
  10 ; neutron pulse repetition (sec)
 100 ; number of runs
```

```
787 ; experiment name
  1 ; max. Line#
-1000 ; delay (msec)
 100 ; channel width
  64 ; number of channels used
  10 ; neutron pulse repetition (sec)
 100 ; number of runs
```

788 ; experiment name  
1 ; max. Line#  
1400 ; delay (msec)  
50 ; channel width  
64 ; number of channels used  
6 ; neutron pulse repetition (sec)  
400 ; number of runs

789 ; experiment name  
1 ; max. Line#  
1400 ; delay (msec)  
50 ; channel width  
64 ; number of channels used  
6 ; neutron pulse repetition (sec)  
600 ; number of runs

790 ; experiment name  
1 ; max. Line#  
1400 ; delay (msec)  
50 ; channel width  
64 ; number of channels used  
6 ; neutron pulse repetition (sec)  
600 ; number of runs

791 ; experiment name  
1 ; max. Line#  
1400 ; delay (msec)  
40 ; channel width  
64 ; number of channels used  
6 ; neutron pulse repetition (sec)  
200 ; number of runs

792 ; experiment name  
1 ; max. Line#  
1400 ; delay (msec)  
40 ; channel width  
64 ; number of channels used  
6 ; neutron pulse repetition (sec)  
200 ; number of runs

793 ; experiment name  
1 ; max. Line#  
1400 ; delay (msec)  
40 ; channel width  
64 ; number of channels used  
6 ; neutron pulse repetition (sec)  
200 ; number of runs

794 ; experiment name  
1 ; max. Line#  
2800 ; delay (msec)  
40 ; channel width  
128 ; number of channels used  
8 ; neutron pulse repetition (sec)  
200 ; number of runs

795 ; experiment name  
1 ; max. Line#  
2800 ; delay (msec)  
40 ; channel width  
128 ; number of channels used  
8 ; neutron pulse repetition (sec)  
200 ; number of runs

796 ; experiment name  
1 ; max. Line#  
2800 ; delay (msec)  
40 ; channel width  
128 ; number of channels used  
8 ; neutron pulse repetition (sec)  
200 ; number of runs

797 ; experiment name  
1 ; max. Line#  
2800 ; delay (msec)  
60 ; channel width  
128 ; number of channels used  
10 ; neutron pulse repetition (sec)  
200 ; number of runs

798 ; experiment name  
1 ; max. Line#  
2800 ; delay (msec)  
60 ; channel width  
128 ; number of channels used  
10 ; neutron pulse repetition (sec)  
200 ; number of runs



## APPENDIX B

### User's manual for program FLW (water flow experiment).

#### B.1. Computer files.

The STARBURST directory DU0:[5,1] (named WATER FLOW) contains the following files necessary for running the experiment:

- FLW.TSK - the task file,
- FLW.ADR - addresses of the modules in the CAMAC crate,
- FLW.STS - actual status parameters for the program.

The FORTRAN program has been prepared in two versions:

- FLWA.FTN - two multiscalers of maximum 128 channels in each one,
- FLWB.FTN - one multiscaler of maximum 256 channels.

Both task files also exist, FLWA.TSK and FLWB.TSK. Version A, copied to the FLW.TSK, has been used during the experiment.

The directory contains also a program which can be run as a test for the work of the created system before starting a series of experiments or in case of an incorrect operation.

The names of the files are

- FLWTST.FTN and FLWTST.TSK .

The directory DU1:[6,2] (the same as for the TD1 data) contains the data files which are created during the experiment:

- \*F0.T1D - raw data from Line #0,
- \*F1.T1D - raw data from Line #1 (if it is used),
- \*F0.T1P - parameters for the TD1 routine,
- \*F0.LOG - log file of the experiment,

where the asterisk denotes the name of the experiment given by the user (usually the measurement number, one to four characters). The log and parameter files are ASCII files, the data files (\*.T1D) are unformatted.

## B.2. Running the experiment.

The program is started by RUN FLW . Then the experiment status is shown (STAND-BY or FINISHED) and depending on it the program asks the user for the experimental parameters. The following data are required for a new experiment:

- Name (usually the experiment number).
- Detector lines to be used (#0, or #0 and #1).
- Delay of the multiscaler start after the neutron pulse (-5000 to 5000 ms),  
the negative sign means that the start of the multiscaler is earlier than of the neutron pulse.
- Channel width (from 40 ms).
- Partition of the total number of channels (e.g. 1/2 or 2/2).
- Repetition of the neutron pulses (0 to 60 s),  
zero means an immediate run after run.
- Number of runs preset,  
can be repeated or changed at a continuation of the experiment.

The user is informed about an available range of any parameter. In most cases at this stage it is possible to abort the program by ^Z.

### *Note!*

The program works in real time during the multiscaler operation. Timing signals come from the STARBURST. Therefore, a high priority is set for the task during the multiscaler run [using the system subroutine, ALTPRI(,100)] and most other actions of the computer are below this priority.

## B.3. Data treatment.

An analysis of the collected data is possible by means of the program TD1 (directory DU0:[6,2] ). The data \*F0 and the parameters \*F0 should be loaded first, to any region of the Histogramic Memory. Then the data \*F1 can be loaded (with no parameters) to another region. Almost all utilities of program TD1 can be used (LOAD, #, UPDATE, PARAMETERS, ANALYZE, INTENSITY, WHERE, MOVE, EXIT). Only BEGIN has to be avoided. If it happened accidentally a new LOAD should be immediately done without any prior SAVE. Generally, SAVE is not recommended although it can be used to save a particular set of the TD1 parameters which have been adjusted during ANALYZE.

*Warning.*

During ANALYZE the peak parameters (the position and the FWHM) are calculated in milliseconds (as indicated at the header of the plot) but a description at the peak picture is apparently in nanoseconds which comes default from the TD1 program which had been prepared for the TANSY analysis.

*Technical note.*

Program TD1 has used the 'PTM' parameter for the total time of the measurement (the 'Active' time). In program FLW the 'PTM' is utilized for the delay time.